Thesis

The role of eukaryotic lipases in pathogen induced cell death.

submitted by

Timo Linder, B.Sc.

in partial fulfillment of the requirements for the degree of

Doktor der gesamten Heilkunde

(Dr. med. univ.)

at the

Medical University of Graz

executed at the

University departments of Diagnostic and Research Institute of Hygiene, Microbiology and Environmental Medicine

under the supervision of **Dr.^{in} rer. nat. Sabine Wagner-Lichtenegger**

and **Univ.-Prof. Dr. med. Ivo Steinmetz**

Graz, 20.12.2024

Declaration of Academic Integrity

I hereby confirm that the present diploma thesis is the result of my own independent scholarly work. I also confirm that in all cases, where material from the work of others (in books, articles, essays, dissertations, and the internet) is acknowledged, quotations and paraphrases are clearly indicated. No material other than that cited in the reference list has been used. I have read and understood the Medical University's regulations and procedures concerning plagiarism.

Furthermore, I hereby declare that if artificial intelligence (AI) tools were used for the generation and/or correction of certain text passages in the creation of this work, such employment was conducted in compliance with ethical principles, academic integrity, and the regulations of my university. Additionally, it was ensured that this usage was transparently disclosed and appropriately attributed.

Graz, 20.12.2024

_____

Timo Linder, B.Sc., m.p.

Acknowledgment

I would like to sincerely thank…

…Dr. Sabine Wagner-Lichtenegger for providing me with an interesting topic for this diploma thesis, her great supervision and guidance during the works of this thesis and her nearly endless input of new ideas.

…Prof. Dr. Steinmetz for the opportunity to execute my diploma thesis at the Diagnostic and Research Institute of Hygiene, Microbiology and Environmental Medicine.

…all the other members of the research team for infection and immunity for their advice, their help and ideas and the always great atmosphere in the lab.

…my friends and family for their support and backing in the ups and downs.

…my girlfriend who made all this possible, always believed in me and stood by my side, especially when things weren't working out as intended.

Zusammenfassung

Diese Arbeit beschäftigt sich mit dem Bakterium *Pseudomonas aeruginosa*, welches zu den wichtigsten Erregern nosokomialer sowie opportunistischer Infektionen gehört.

Auf dem zellulären Level kann eine Infektion mit *P. aeruginosa* unterschiedliche Arten von Zelltod in eukaryotischen Zellen auslösen. Zwei dieser Zelltodmechanismen sind Ferroptose und Pyroptose, lytische Zelltodmechanismen, die zu einer Entzündungsreaktion führen. Im Vordergrund dieser Arbeit steht Ferroptose, ein Mechanismus, welcher nicht nur von der Anwesenheit von Eisen abhängt, sondern im Speziellen auch von der Akkumulation peroxidierter Lipide. Diese peroxidierten Lipide führen zur Lyse der Zelle. Einige virulente *P. aeruginosa* Stämme exprimieren Exotoxin U, eine bakterielle Lipase, welche Ferroptose unter Anwesenheit peroxidierter Lipide verstärken kann. Die Zusammensetzung dieser Lipide hängt unter anderem von der Aktivität bestimmter Enzyme, Lipasen, ab. Die Rolle von eukaryotischen Lipasen für die *P. aeruginosa* abhängige Induktion einer Ferroptose ist allerdings bisher nicht erforscht. Die Hypothese dabei wäre, dass eine Inhibition der Lipasen zu einer veränderten Lipidzusammensetzung in der Zelle führt, welche wiederum Auswirkungen auf die Ferroptose Induktion hat. Daher beschäftigt sich diese Arbeit mit der Charakterisierung des *P. aeruginosa* induzierten lytischen Zelltodes und der Auswirkungen der Inhibition unterschiedlicher eukaryotischer Lipasen auf diesen. Daraus könnten sich neue therapeutische Optionen im Rahmen der Wirt-gerichteten Therapie bei infektiösen Erkrankungen ergeben.

Dazu wurde zunächst ein Infektionsassay etabliert, mit welchem sich Lyse in eukaryotischen Zellen nachweisen lässt. Von den analysierten Zelltypen zeigten THP1-Zellen, ein Modellsystem für humane Makrophagen, die stärkste Lyse bei Infektion mit *P. aeruginosa*, sowie weiteren Bakterien (*Burkholderia thailandensis*, *Burkholderia pseudomallei* sowie *Escherichia coli*). Durch Hemmung der Ferroptose mittels Ferrostatin-1 wurde der beobachtete lytische Zelltod allerdings nicht unterdrückt. Eine Deletion der Caspase-1, einem Pyroptose induzierendem Enzym, führte zur Reduktion der Zelllyse. Weiters führte eine Inhibierung unterschiedlicher Lipasen zu keiner veränderten Zelllyse. Diese Ergebnisse weisen darauf hin, dass es sich bei dem primär ausgelösten Zelltod in unserem Modell um Pyroptose handelt, die, wie unsere Ergebnisse zeigen, unabhängig von den hier getesteten Lipase-Inhibitoren ist.

Abstract

This thesis deals with the bacterium *Pseudomonas aeruginosa*, which is one of the most important pathogens of nosocomial and opportunistic infections.

At the cellular level, infections with *P. aeruginosa* trigger different types of cell death in eukaryotic cells. Two of these cell death mechanisms are ferroptosis and pyroptosis, which lead to an inflammatory reaction. The focus of this work is ferroptosis, a mechanism that depends not only on the presence of iron, but in particular also on the accumulation of peroxidized lipids. These peroxidized lipids lead to lysis of the cell. Some virulent *P. aeruginosa* strains express exotoxin U, a bacterial lipase that can enhance ferroptosis in the presence of peroxidized lipids. The composition of these lipids depends, among other things, on the activity of certain enzymes, eukaryotic lipases. However, the role of eukaryotic lipases in the *P. aeruginosa*-dependent induction of ferroptosis has not yet been investigated. The hypothesis is that inhibition of lipases leads to an altered lipid composition in the cell, which in turn influences ferroptosis induction. Therefore, this thesis deals with the characterization of *P. aeruginosa* induced lytic cell death and the effects of the inhibition of different eukaryotic lipases on it. This could lead to new therapeutic options in the context of host-directed therapy for infectious diseases.

To this end, an infection assay was first established with which lysis can be detected in eukaryotic cells. Of the cell types analyzed, THP1 cells, a model system for human macrophages, showed the strongest lysis when infected with *P. aeruginosa*, as well as other bacteria (*Burkholderia thailandensis*, *Burkholderia pseudomallei* and *Escherichia coli*). However, applying ferrostatin-1 did not suppress the observed lytic cell death. The deletion of caspase-1, a pyroptosis-inducing enzyme, resulted in a reduction of cell lysis. Moreover, the inhibition of various lipases did not result in any alterations in cell lysis. These results indicate that the primary induced cell death in our model is pyroptosis, which, as our results show, is independent of the lipase inhibitors tested.

Table of contents

Abbreviations

Abbreviation	Explanation
°C	Degrees Celsius
2-AG	2-Arachidonoylglycerol
ABHD6/ABHD12	Alpha/Beta-hydrolase domain containing 6/12
ACK	Ammonium-Chloride-Potassium
ATGL	Adipose triglyceride lipase
BAK	Bcl-2 homologous antagonist/killer
BAX	BCL2 associated X protein
BCL-2	B-cell lymphoma 2
CB	Cannabinoid (receptor)
CF	Cystic fibrosis
CFU	Colony forming units
COPD	Chronic obstructive pneumonic disease
DAG	Diacylglycerol
DAMP	Damage-associated molecular pattern
demin.	Demineralized
DMSO	Dimethyl sulfoxide
DNA	Desoxyribonucleic acid
EDTA	Ethylenediaminetetraacetic acid
e.g.	Exempli gratia
EGTA	Ethylene glycol-bis (β-aminoethyl ether)-N,N,N‘,N‘-tetraacetic acid
ExoU	Exotoxin U
F-12K	F-12 Kaighn’s
FBS	Fetal bovine serum
g	Gram
g	G-forces
G	Gauge
GM-CSF	Granulocyte-macrophage colony-stimulating factor
GPX4	Glutathione peroxidase 4
GSH	Glutathione
h	Hour
hMDM	Human monocyte derived macrophages
•HO	Hydroxyl radical
HSL	Hormone-sensitive lipase
IL	Interleukin
IPTG	Isopropyl β-D-1-thiogalactopyranoside
L	Liter
LB	Lysogeny broth

LDH	Lactate-Dehydrogenase
LPS	Lipopolysaccharide
M	Molar
M-CSF	Macrophage colony-stimulating factor
MAG	Monoacylglycerol
MAGL	Monoacylglycerol lipase
mg	Milligram
MGL	Monoacylglycerol lipase
min	Minutes
mL	Milliliter
mM	Millimolar
mMDM	Murine monocyte derived macrophages
MOI	Multiplicity of infection
ng	Nanogram
NLR	NOD-like receptor
nm	Nanometer
NOD	Nucleotide-binding oligomerization domain
ns	Not significant
OD_{600nm}	Optic density at 600 nm
PAMP	Pathogen-associated molecular pattern
PBS	Phosphate buffered saline
PCR	Polymerase chain reaction
PMA	Phorbol 12-myristate 13-acetate
PUFA	Polyunsaturated fatty acid
rhu	Recombinant human
rm	Recombinant murine
RPMI 1640	Roswell Park Memorial Institute 1640
sec	Second
T3SS	Type 3 secretion system
TAE	Tris-acetate-EDTA
TAG	Triacylglycerol
TNF-α	Tumor necrosis factor α
TP53	Tumor protein P53
UTI	Urinary tract infection
UV	Ultraviolet
w/o	Without
WHO	World Health Organization
Xc-	Cystine/glutamate transporter
µg	Microgram
µL	Microliter
µM	Micromolar

1. Introduction

1.1 Microbial pathogens

Pathogens in their broadest and most general sense are microorganisms that can cause diseases. Among those microorganisms there are different types, such as viruses, protozoa, prions, viroid, fungi and bacteria [1]. Human pathogens are pathogens which cause different diseases and illnesses when invading the human body. Those pathogens infiltrate the body by different pathways and trigger various symptoms and diseases via many miscellaneous mechanisms. Among these mechanisms there are e.g. the lytic and lysogenic cycle of viruses or the release of endo- and exotoxins by for example bacteria [2-4].

A large proportion of pathogens falls back on pathogenic bacteria. Although most species of bacteria are no threat to human health but instead sometimes even beneficial, there are also many species that can cause diseases and severe illness in the human organism [5].

Those diseases vary over a wide range, from minor or even harmless skin infections to life-threatening conditions like sepsis or tuberculosis [5]. Pathogenic bacteria employ various strategies to colonize and damage their hosts. Some produce virulence factors such as adhesins that facilitate attachment to host cells, while others secrete enzymes that degrade host tissues or toxins that disrupt normal cellular functions [6]. Therefore, the study of those pathogenic bacteria is crucial in microbiology and infectious disease research. Understanding the mechanisms of bacterial pathogenicity and the factors that contribute to antibiotic resistance is essential for developing effective treatments and preventive measures. Continued research in bacterial pathogenesis, host-pathogen interactions, and the development of novel antimicrobial agents remains a top priority in the fight against bacterial diseases [7].

1.1.1 *Pseudomonas aeruginosa* as a human pathogen

One of those aforementioned pathogenic bacteria is *Pseudomonas aeruginosa*, a Gram-negative, rod-shaped and flagellated bacterium, which was isolated for the first time by the French pharmacist Carle Gessard in 1882 [8]. *P. aeruginosa* is found primarily in soil, water or other wet or moist milieus and is facultative anaerobic [9].

Due to its ubiquity and intrinsically advanced multidrug resistance, it is considered as an organism of high medical importance, reaching the "WHO priority list for antibiotic resistant bacteria" [10, 11]. *P. aeruginosa* is most commonly associated with respiratory infections such as pneumonia [12, 13], but also known to infect other systems of the human body, such as the urinary tract (e.g. UTIs), skin and soft tissue (e.g. on burns or contaminated wounds) or the digestive system (e.g. necrotizing enterocolitis) [14]. It plays an important role in nosocomial infections being one of the most common nosocomial germs and leading to serious symptoms and illnesses [15]. *P. aeruginosa* is also considered an opportunistic pathogen as its infestations often follow existing diseases. Hereby the most notably are cystic fibrosis (CF) and chronic obstructive pneumonic disease (COPD) [16, 17].

Via the type III secretion system (T3SS) some strains of *P. aeruginosa* secrete the Exotoxin U (ExoU) which is an important virulence factor and for instance increases mortality in CF-patients significantly [18, 19]. ExoU possesses a patatin-like phospholipase A2 activity that can trigger lysis of the host cell, e.g. macrophages, neutrophile granulocytes or epithelial cells, through ferroptosis, an iron dependent cell death mechanism that will be explained in the following section [19-24]. Briefly, lipid peroxidation activates ExoU, which in turn induces cell lysis dependent on its phospholipase activity [20-25].

1.1.2 ExoU in *Burkholderia pseudomallei* and *Burkholderia thailandensis*

Another bacterium that secretes ExoU via the T3SS are *Burkholderia pseudomallei* and *Burkholderia thailandensis*, Gram-negative, rod-shaped and flagellated bacteria which were firstly described in 1993 and 1998 [26-28]. Both are also mostly found in soil and are close relatives [29]. Compared with *B. pseudomallei* which causes the infectious disease melioidosis, *B. thailandensis* is much less pathogenic, showing a lethal inoculum 1,000 times higher than *B. pseudomallei* [30]. Due to its close relation but much lesser pathogenic potential, *B. thailandensis* is often used as a model organism for *B. pseudomallei* since results from the study of this bacterium are often translatable to the more pathogenic organism [27, 30, 31].

1.2 Eukaryotic cell death mechanisms

When looking at cell death mechanisms one must differ between two main subcategories of cell death. On the one hand there is programmed cell death which is mediated by intracellular programs carried out in regulated processes [32]. Those processes vary in their pathways. On the other hand, there is necrotic cell death which is triggered by external forces like trauma or infections that lead to swelling and consequently rupture of the cell membrane.

1.2.1 Necrosis

In contrast to programmed cell deaths, necrosis does not follow a specific pathway like apoptosis or other forms of regulated cell death. Instead, a cell injury, e.g. occurring in the form of trauma, infection or inflammation, leads to a loss of integrity in the cell membrane. Hereby a noxious stimulus triggers the opening of ion-channels, allowing extracellular ions and thereby fluid to flood the cells' inner structure. This causes the cell to swell and results inevitably in the membrane to rupture which is followed by spillage of the cells internal contents and further tissue damage in the surroundings. [33-36]

1.2.2 Apoptosis

Apoptosis is probably the most well-known form of programmed cell death. Being a highly regulated process, it leads to an inevitable death of the cell [37]. While there are two different initial pathways that induce apoptosis, both result in an activation of caspases, divided into initiator and effector caspases.

The intrinsic pathway is activated under certain kinds of stress that the cell is exposed to, e.g. hypoxia, DNA damage or chemotherapeutic agents. It starts with an oligomerization of BAK and BAX, two BCL-2 proteins, which leads to pore formation in the mitochondrial membrane. These pores allow cytochrome C to be released into the cytosol and bind to apoptosis protease factor 1 and thereby recruit caspase-9. The now formed apoptosome cleaves the caspase-9 proteolytically which initiates the caspase processing cascade. [38]

The extrinsic pathway on the other hand is activated when death signals from other cells reach the cell. Ligands then bind to specific receptors on the membrane surface and initiate

different pathways via distinct mediators, such as TNF-α, Fas, *Bcl-2* genes or *TP53* suppressor gene. Those mediators conduct their own pathway, all of them resulting in the activation of the caspase cascade. For example, TNF-α binds the TNF receptor and forms the TNF receptor associated death domain (TRADD) that then activates procaspase-8. The activated caspase-8 now triggers the activation of the caspase cascade. [38, 39]

The caspase cascade is a complex pathway where initiator caspases (e.g. caspase-9, -10) activate effector caspases (e.g. caspase-3, -6) by cleavage revealing their executioner function. This leads to multiple effects inside the cell such as cleaving of certain intracellular proteins, membrane blebbing and degradation of genomic DNA. The cell starts to shrink and finally breaks apart into multiple vesicles that undergo phagocytosis. [38]

1.2.3 Ferroptosis and pyroptosis

Pyroptosis and ferroptosis on the one hand are regulated or programmed just like apoptosis and each follow a specific pathway. On the other hand, they lead to a disintegration of the cell's membrane resulting in an uncontrolled release of the cell contents, like necrosis. Those cell death mechanisms are therefore called non-apoptotic regulated cell deaths. [40-42]

Ferroptosis, previously known as oxytosis, is one of those special kinds of cell death and is described as an "iron-dependent cell death characterized by accumulation of lipid peroxides" [43, 44]. Via the Fenton-Reaction, iron facilitates the formation of reactive oxygen species. Hereby, hydrogen peroxide (H_2O_2) is converted to hydroxyl radicals ($^{\bullet}HO$) that contribute to lipid peroxidation [45]. The accumulation of these lipid peroxides, or peroxidized polyunsaturated fatty acids (PUFAs), is the hallmark of ferroptosis. The lipids compromise the integrity of the cell membrane which leads to its disintegration and therefore the lysis of the cell [43, 44, 46]. Key regulators of ferroptosis include glutathione peroxidase 4 (GPX4), which detoxifies lipid peroxides, and the glutathione (GSH)-dependent system Xc-, a cystine/glutamate antiporter essential for maintaining cellular antioxidant defenses [47]. Due to its occurrence in different pathological processes, ferroptosis has been hypothesized to be a potential target for various medical fields, such as in cancer therapy, the treatment of neurodegenerative diseases and also in inflammation and infectious diseases [48-51].

Pyroptosis is another form of lytic cell death, mostly associated with infection by intracellular pathogens [52]. Intracellular pathogens like bacteria are recognized by the inflammasome complex, a cytosolic multiprotein complex that senses microbe-derived pathogen-associated molecular patterns (PAMPs) and damage-associated molecular patterns (DAMPs) via NOD-like receptors (NLRs) [34, 53-55]. Subsequently the inflammasome activates caspase-1 via proteolytical cleavage, which itself further cleaves pro-inflammatory cytokines (interleukins IL-1β and IL-18) and the protein gasdermin-D. The N-terminal domain of gasdermin-D then perforates the cell's membrane by forming pores that cause swelling and hereby lytic cell death [56, 57]. While this is called the canonical inflammasome pathway, there is also the noncanonical inflammasome pathway. In the noncanonical pathway, bacterial lipopolysaccharides (LPS) are recognized directly by caspase-4/5 (humans) or -11 (mice), which initiate pyroptosis. While caspase-4/5 cannot cleave the proforms of IL-1β and IL-18, they still cleave gasdermin-D and therefore trigger pyroptosis [56, 58].

1.3 The role of lipids in cell death

Lipids and their metabolism play an important role in different mechanisms of cellular death. They act as mediators, modulate the properties of membranes they are embedded in as well as enhancing cell death by modulating affinities between executors and regulators [59-63].

In apoptosis for example, mitochondrial lipids form the structural foundation of the proteolipidic apoptotic pore [64-66].

Regarding this thesis, the most important factor of lipid influence on cell death, however, is their role in ferroptosis. In ferroptosis the main hallmark is the accumulation of peroxidized lipids [44, 59]. Membrane phospholipids containing PUFAs, such as arachidonic acid, are particularly susceptible to such peroxidation, which makes them an ideal target in the ferroptotic process [47, 67, 68]. It is known that the peroxidation of especially phospholipids targets all cellular membranes such as the mitochondrial membrane, the plasma membrane or the endoplasmic reticulum. Meanwhile the details and the specific targets of those molecular mechanisms of ferroptotic cell death remain to be explored [69]. Currently, there is no evidence indicating whether ferroptosis involves protein-based or

lipid-based pores, and research is ongoing. One hypothesis suggests that oxidative damage may cause small gaps in the plasma membrane, disrupting ion homeostasis. It is unclear whether PUFA lipid peroxidation during ferroptosis alone causes membrane permeabilization or alters membrane properties affecting key proteins' functions [59, 69]. Arachidonic acid does not only play a significant role in the ferroptotic process but also in other aspects regarding infection and inflammation. On the one hand it is a predecessor of various lipid mediators, like the eicosanoid derived prostaglandins, and other inflammatory mediators [70]. On the other hand, its ester with glycerol, 2-arachidonoylglycerol (2-AG) is an endocannabinoid and acts as an endogenous agonist on the cannabinoid 1 receptor (CB_1) and the primary endogenous ligand for the CB_2 receptor. This binding is followed by various anti-inflammatory effects such as the inhibition of proinflammatory cytokines, analgesia and regulation of intracellular Ca^{2+}-levels [71, 72]. It can be concluded from this that the study of lipids in connection with both cell death mechanisms and inflammatory reactions is certainly relevant for further research into these mechanisms and relationships.

1.4 The influence of lipases

When talking about lipids one important factor that must be considered are lipases. Enzymes that cleave lipids and the metabolism of lipids via those enzymes are strongly linked together and cannot be viewed separately. Regarding the topics infection and thereby ferroptosis and pyroptosis, important lipases are eukaryotic lipases, since ferroptosis only occurs in eukaryotic cells [34]. Pyroptosis was long believed to do so as well but was recently shown to also occur in bacteria [73].

1.4.1 Lipolysis – the degradation of triglycerides

Lipases in general are enzymes that catalyze the hydrolysis of lipids and their descendants, classically hereby is the degradation of triglycerides. The degradation process of triglycerides (Triacylglycerol – TAG), or lipolysis, consists of three major steps. At first, the TAG gets hydrolyzed via a triglyceride lipase such as adipose triglyceride lipase (ATGL), hereby one of the three fatty acids gets split off, leaving a diacylglycerol (DAG). This DAG

subsequently gets hydrolyzed by a diacylglycerol lipase like hormone-sensitive lipase (HSL), again splitting off a fatty acid chain and therefore a monoacylglycerol (MAG) remains. The MAG now goes through one last step of hydrolyzation via a monoacylglycerol lipase (MGL), cleaving it into one fatty acid chain and one glycerol molecule. This process is illustrated below in Figure 1. [74-76]

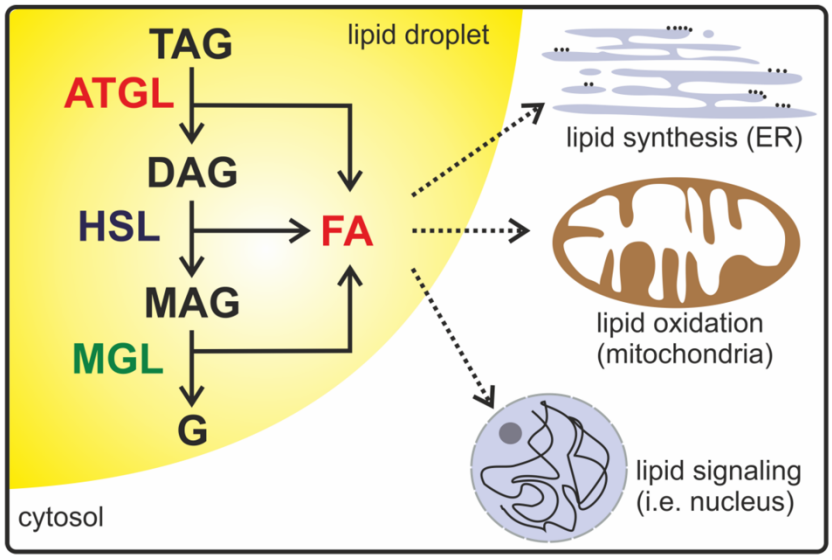

Figure 1: **The three steps of lipolysis.** In lipolysis triglycerides get degraded to glycerol and fatty acids by three steps. Firstly, the TAG gets hydrolyzed via a triacylglycerol lipase (ATGL) to a fatty acid and diacylglycerol. The DAG gets further hydrolyzed by a diacylglycerol lipase (HSL) to monoacylglycerol and a fatty acid. In the third step, MAG gets hydrolyzed one last time by monoacylglycerol lipase (MGL) to glycerol and a fatty acid. Those fatty acids that result from this process can be used later in different operations like lipid synthesis, lipid oxidation or lipid signaling. The figure was obtained from Hofer, P. *et al.*, "The Lipolysome – A Highly Complex and Dynamic Protein Network Orchestrating Cytoplasmic Triacylglycerol Degradation." Metabolites, 2020. 10(4). [75]

1.4.2 The Lipases ATGL, ABHD6 and MAGL

The examined lipases in this thesis are the adipose triglyceride lipase (ATGL), the alpha/beta-Hydrolase domain containing 6 (ABHD6) and the monoacylglycerol lipase (MAGL).

ATGL is a triacylglycerol lipase catalyzing the first step of lipolysis and consists of a catalytic dyad of serine-aspartic acid [76-78]. Since ATGL catalyzes the initial reaction it acts as a control mechanism of lipolysis with variations in its activity lead to alternated levels of DAG, subsequently affecting further steps [79]. Emerging from this, elevated levels of TAG can cause neutral lipid storage disease by the accumulation of TAG-droplets in neutrophils [80]. Besides its lipase activity in lipolysis, ATGL also possesses a phospholipase activity, cleaving

e.g. phospholipids of the plasma membrane [81]. ATGL can be inhibited artificially and selective by the statin atglistatin [82].

ABHD6, also known as 2-arachidonoylglycerol hydrolase, is a monoacylglycerol lipase, executing the third step of lipolysis, cleaving MAGs into their fatty acid chain and the glycerol molecule [83]. As its name suggests, ABHD6 has a specific affinity to 2-AG and is therefore closely linked to the endocannabinoid system, controlling the degradation and hereby also the accumulation of 2-AG at the cannabinoid receptors [84]. Especially in the brain ABHD6 plays an important role, accounting for roughly 4% of 2-AG hydrolysis [85]. In human macrophages this proportion is even higher [86]. The enzyme can be inhibited artificially and selective by different inhibitors, such as KT182 and WWL70 [87, 88].

MAGL is another monoacylglycerol lipase, converting MAGs to their fatty acid chain and one glycerol molecule. Together with ABHD6 it is a key enzyme in the regulation of 2-AG, covering about 85% of 2-AG hydrolysis in the human brain and combined with ABHD6 and ABHD12 cumulating to 99% [89]. To induce 2-AG accumulation, MAGL can be inhibited by several inhibitors such as URB602, URB754 and JZL184 [90].

1.5 Aims of this thesis

The infection of eukaryotic cells with bacteria like *P. aeruginosa* or *B. thailandensis* can lead the cells into non-apoptotic cell deaths such as ferroptosis or pyroptosis. Specifically, ferroptosis is known for its dependence not only on the presence of iron, but also, as its hallmark, the accumulation of peroxidized PUFAs or other peroxidized lipids. One of these PUFAs is arachidonic acid, a descendant of 2-arachidonoylglycerol. The peroxidized lipids then lead to an integrity loss of the cell membrane and therefore to its disintegration. Lipids, including those playing a role in ferroptosis, are regulated and cleaved by various enzymes, named lipases. Three of these lipases are the tri- and monoacylglycerol lipases ATGL, ABHD6 and MAGL.

The aim of this thesis was to examine the influence of those lipases in relation to ferroptosis and other eukaryotic cell deaths. Therefore, cells were infected with the ExoU secreting clinical sample of *P. aeruginosa* CF1013. The hypothesis was that an inhibition of those lipases might cause a decrease in arachidonic acid, an important target in ferroptosis, and therefore reduce lysis in eukaryotic cells by taking away the “fuel” for ExoU-dependent ferroptosis. Additionally, an increase in 2-AG was shown to have anti-inflammatory effects. Another effect would be a decrease in cell lysis by inhibiting ATGL, which holds a phospholipase activity. These hypotheses would then identify eukaryotic lipases as potential new targets for host-directed therapy in infectious and inflammatory diseases by decreasing the pro-inflammatory and potentially harmful cell death, ferroptosis.

2. Material and Methods

2.1 Material

2.1.1 Bacterial strains, cells and cell lines

Bacterial strains and cell lines used in this thesis are listed in Table 1 and Table 2, respectively. Bacterial strains were stored in LB-medium, containing 20% glycerol, at -80 °C. Cell lines were stored in cryovials in liquid nitrogen at -180 °C.

Table 1: Bacterial strains used in this thesis.

Strain	Description	Reference
P. aeruginosa	CF1013	Clinical isolate, obtained at the institute for Hygiene, Microbiology and Environmental Medicine, Medical University of Graz.
B. thailandensis	E264	Type strain [26].
E. coli	DHB5α (pET15b/ExoU)	Gift from Zimmermann Lab, University of Graz.

Table 2: Cell lines used in this thesis.

Cell lines	Description	Reference
A549	Human alveolar epithelial cells, obtained from lung cancer tissue.	ATCC [91, 92].
THP1	Human monocytic cell line from an acute monocytic leukemia patient.	InvivoGen [93, 94].
THP1-*defCasp1*	THP-1 cells with caspase-1 deficiency.	InvivoGen [95, 96].

2.1.2 Chemicals and devices

All chemicals and devices, which were used in this thesis are listed in Table 3 and Table 4, respectively.

Table 3: List of chemicals used in this thesis.

Chemical	Manufacturer
Acridine Orange Stain	Logos, Biosystems, Villeneuve d'Ascq, FR
Agar-Agar, Kobe I	Carl Roth GmbH & Co. KG, Karlsruhe, D
Agarose Standard	Carl Roth GmbH & Co. KG, Karlsruhe, D
Ambion™ nuclease-free Water	Thermo Fisher Scientific, Waltham, MA, USA
Density gradient medium – Lymphoprep	StemCell Technologies Inc., Vancouver, CA
Gibco™ Trypsin-EDTA	Thermo Fisher Scientific, Waltham, MA, USA
Glycerin	Carl Roth GmbH & Co. KG, Karlsruhe, D
Midori Green Advance DNA Stain	NIPPON Genetics EUROPE, Düren, D
Q5® High GC Enhancer	New England Biolabs® Inc., Ipswich, MA, USA
Q5® Reaction Buffer Pack (5x)	New England Biolabs® Inc., Ipswich, MA, USA
RosetteSep Human Monocyte Enrichment Cocktail	StemCell Technologies Inc., Vancouver, CA
6x DNA Loading Dye	Thermo Fisher Scientific, Waltham, MA, USA

Table 4: List of devices used in this thesis.

Device	Type	Manufacturer
BBD 6220	Incubator	Thermo Fisher Scientific, Waltham, MA, USA
BioShake iQ	Heating block	Qinstruments GmbH, Jena, D
Centrifuge 5415 R	Centrifuge	Eppendorf AG, Hamburg, D
Centrifuge 5424 R	Centrifuge	Eppendorf AG, Hamburg, D
Centrifuge 5810 R	Centrifuge	Eppendorf AG, Hamburg, D
CryoCube F570hw	ULT Freezer	Eppendorf AG, Hamburg, D
Dri-Block®	Heating block	VWR International GmbH, Darmstadt, D

DU-640	Spectrophotometer	Beckman Coulter, Brea, CA, USA
GelDoc Go	Gel imaging system	Bio-Rad Laboratories, Hercules, CA, USA
Hera cell 150	Incubator	Thermo Fisher Scientific, Waltham, MA, USA
Hera safe KS	Safety workbench	Thermo Fisher Scientific, Waltham, MA, USA
Lab Dancer®	Vortex-shaker	VWR International GmbH, Darmstadt, D
Luna FX7	Fluorescence cell counter	Logos, Biosystems, Villeneuve d'Ascq, FR
Orbital Shaker-incubator ES-20	Orbital shaker/incubator	BioSan, Riga, LV
Qubit 4	Fluorometer	Thermo Fisher Scientific, Waltham, MA, USA
RCT basic	Magnetic stirrer	IKA-Werke, Staufen im Breisgau, D
ROTILABO® Mini centrifuge	Centrifuge	Carl Roth GmbH & Co. KG, Karlsruhe, D
Safe 2020	Safety workbench	Thermo Fisher Scientific, Waltham, MA, USA
Sigma 4-16KS	Centrifuge	Sigma Laborzentrifugen GmbH, Osterode am Harz, D
Standard Power Pack P25 T	Power pack	Analytik Jena GmbH+Co. KG, Jena, D
T 3000	Thermocycler	Analytik Jena GmbH+Co. KG, Jena, D
TIN-IN120	Incubator	Phoenix Instruments, Garbsen, D
UVT-B-AR	UV-Workbench	BioSan, Riga, LV

2.1.3 Kits and enzymes

Kits and enzymes used in this thesis as well as their manufacturers are listed below in Table **5** and Table 6, respectively.

Table 5: Kits used in this thesis.

Kit	Manufacturer
CytoTox-One homogenous membrane integrity assay	Promega Corp., Madison, WI, USA
NightXpress Mix2Seq Kit	Eurofins Genomics Europe Shared Services GmbH, Ebersberg, D
NucleoSpin Microbial DNA Mini kit for DNA from microorganisms	Macherey-Nagel, Düren, D
Wizard® SV Gel and PCR Clean-Up System	Promega Corp., Madison, WI, USA

Table 6: Enzymes used in this thesis.

Enzyme	Manufacturer
Q5® High-Fidelity DNA Polymerase	New England Biolabs® Inc., Ipswich, MA, USA

2.1.4 Inducers and inhibitors

The inducers and inhibitors used in this thesis as well as their manufacturer are listed in Table 7.

Table 7: Inducers and inhibitors used in this thesis.

Inducers and inhibitors	Manufacturer
Atglistatin (30 mM)	Sigma-Aldrich, Vienna, AT
Ferrostatin-1 (20 mM)	Sigma-Aldrich, Vienna, AT
JZL 184 (1 mM)	Sigma-Aldrich, Vienna, AT
KT 182 (1 mM)	Sigma-Aldrich, Vienna, AT
rhuGM-CSF (100 µg/mL)	PeproTech by Thermo Fisher Scientific, Waltham, MA, USA
rhuM-CSF (10 µg/mL)	PeproTech by Thermo Fisher Scientific, Waltham, MA, USA
rmM-CSF (10 µg/mL)	PeproTech by Thermo Fisher Scientific, Waltham, MA, USA

2.1.5 Oligonucleotides

The oligonucleotides used in this thesis are listed in Table 8.

Table 8: Oligonucleotides used in this thesis.

Name	Base sequence (5'-3')	Reference
ExoU_fw	GCTAAGGCTTGGCGGAATA	[97]
ExoU_rv	AGATCACACCCAGCGGTAAC	[97]

2.1.6 Media, supplements and buffer

The media, supplements and buffer used in this thesis as well as their manufacturers are listed below in Table 9, Table 10 and Table 11, respectively. For agar plates, 15 g/L agar was added to the media components.

Table 9: Media used in this thesis.

Medium	Manufacturer
Gibco™ RPMI 1640	Thermo Fisher Scientific, Waltham, MA, USA
Gibco™ F-12K	Thermo Fisher Scientific, Waltham, MA, USA
LB-premix	Carl Roth GmbH & Co. KG, Karlsruhe, D

LB-Medium	
Substance	**Concentration**
LB-premix	20 g/L
demin. H_2O	

This media was autoclaved at 121 °C for 20 minutes (min). Antibiotics and other supplements were sterile filtered and added after autoclaving.

Table 10: Supplements used in this thesis.

Supplement	Manufacturer
Ampicillin (50 mg/mL)	Sigma-Aldrich, Vienna, AT
DMSO	Sigma-Aldrich, Vienna, AT
EGTA 0,5 M, pH 8,0	Thermo Fisher Scientific, Waltham, MA, USA
Fetal Bovine Serum (FBS)	Thermo Fisher Scientific, Waltham, MA, USA

Gibco® 2-mercaptoethanol	Thermo Fisher Scientific, Waltham, MA, USA
Human Serum	Sigma-Aldrich, Vienna, AT
Hygromycin B Gold (100 mg/mL)	InvivoGen, San Diego, CA, USA
Normocin (50 mg/mL)	InvivoGen, San Diego, CA, USA

Table 11: Buffer used in this thesis.

Buffer	Manufacturer
ACK lysis buffer	Thermo Fisher Scientific, Waltham, MA, USA
DPBS (10X) w/o Ca and Mg	PAN-Biotech GmbH, Aidenbach, D
Gibco™ PBS pH 7,4	Thermo Fisher Scientific, Waltham, MA, USA
ROTIPHORESE® 50x TAE Buffer	Carl Roth GmbH & Co. KG, Karlsruhe, D

2.2 Methods

2.2.1 Microbiological methods

2.2.1.1 Cultivation of bacteria

All used bacteria were cultivated using LB-medium. From a glycerol culture one inoculation loop was spread out on an agar plate and grown overnight at 37 °C. On the next day one colony was picked and inoculated into a 100 mL shaking flask, containing 20 mL of LB-medium as well as the respectively used additives. The culture was again grown overnight. The third day, when the assay was performed, the culture was diluted 1:50 and grown until an OD_{600nm} of 1 [20]. Used additives were 100 µg/mL ampicillin and 1 mM IPTG for *E. coli* DHB5α (pET15b/ExoU) and 10 mM EGTA for *P. aeruginosa* CF1013.

2.2.1.2 Preparation of infection medium

For the infection assay the culture was centrifuged at 5,000 rpm for 5 min at room temperature, washed once with PBS and adjusted to an OD_{600nm} of 1. To achieve the desired MOI, the appropriate volume of bacteria suspension was added to the cell culture medium, calculated by the dilution formula. At an OD_{600nm} of 1, *P. aeruginosa* showed

4.54x10^8 CFU/mL, *B. thailandensis* showed 6.26x10^8 CFU/mL and *E. coli* showed 3.63x10^8 CFU/mL.

To determine the exact MOI for each assay, a dilution series of the infection mix was performed on LB-agar plates. The MOI was calculated by counting the colonies and using Equation 1.

Equation 1: Calculation of the true MOI used in an infection mix.

$$MOI = \frac{\text{number of colonies x dilution x volume per well}}{\text{seeded cells per well x plated volume}}$$

If needed, additives were added to the infection mix in corresponding concentrations as mentioned in the chapter Results.

For preincubation and after the infection, only the additives were added to the cell culture medium, without any bacteria

2.2.1.3 Infection assay

If indicated, cells were pre-incubated with a corresponding pre-incubation mix for 2 hours (h) at 37 °C with 5% CO_2 and 95% humidity. Afterwards, the pre-incubation mix was removed, and the infection mix was added to the wells. After an incubation of the plate for 30 min at 37 °C with 5% CO_2 and 95% humidity, the infection mix was removed, and the wells were washed twice with PBS-buffer. Subsequently only medium, with additives and without bacteria, was added to the wells and again incubated for 30 min at 37 °C with 5% CO_2 and 95% humidity. Time point zero was defined as half an hour after the post-incubation medium was added to the cells. For subsequent time points the sole medium with additives was left on respectively.

At sample collection, 150 µL of the supernatant were used for CFU determination of extracellular bacterial load. The remaining supernatant was frozen at -80 °C for later use in a cytotoxicity assay. [56]

2.2.1.4 CFU determination of extracellular bacterial load

For the determination of the extracellular bacterial load, 150 µL of the supernatant were diluted in a dilution series up to 10^{-5}. Afterwards 20 µL of each dilution were plated onto

LB-agar plates and incubated at 37 °C for 24-48 h. The CFU was then calculated by counting the grown colonies and using Equation 2.

Equation 2: Calculation of the extracellular CFU/mL after post infection.

$$\text{CFU/mL} = \text{number of colonies on plate x dilution x } 50$$

2.2.2 Cell culture methods

2.2.2.1 Human monocyte derived macrophages (hMDM)

2.2.2.1.1 Ethic statement

Primary human monocytes were isolated from blood donated by healthy individuals during a platelet apheresis procedure. Donors were anonymized and provided written consent for their blood to be used. This consent included the use of their blood in basic research and was approved by the Ethical Review Committee of the Medical University of Graz (No. 34-515 ex 21/22). [56]

2.2.2.1.2 Isolation of monocytes

The isolation of human monocytes was performed by other members of the institute. Briefly, after the blood donation, blood was obtained from the leukocyte depletion chamber and 13 mL PBS were used to flush the chamber. Then 1 mM EDTA was added to avoid clumping of the blood. 50 µL of RosetteSep Enrichment Cocktail were added per mL of blood/PBS mixture and gently mixed. After incubation at room temperature for 20 min, the mixture was aliquoted into 5 mL samples to four centrifuge tubes and 15 mL PBS containing 2% FBS and 1 mM EDTA were added each and mixed gently again. Then 15 mL Lymphoprep were added, and the suspension was centrifuged at 12,000 g for 20 min. After the transfer of the enriched monocyte rings into new tubes, the suspension was filled to 50 mL with PBS containing 2% FBS and 1 mM EDTA and centrifuged again at 300 g for 10 min. 10 mL of PBS containing 2% FBS and 1 mM EDTA were used to suspend the pellet and two tubes were combined. After two further washing steps, each combining two tubes again, the resulting pellet was suspended in RPMI 1640 medium with 10% human serum and the cell number was determined. At a final concentration of $1x10^7$ cells/mL with 10% DMSO, $1.7x10^7$ cells were transferred to cryotubes and slowly frozen, using a

Mr. Frosty freezing container for 24 h at -80 °C. The isolated monocytes were stored in liquid nitrogen. [56]

2.2.2.1.3 Differentiation to human macrophages

To differentiate the human monocytes to human monocyte derived macrophages (hMDMs), the isolated monocytes were thawed in a 37 °C water bath and washed with 20 mL of warm RPMI + 10% human serum. After centrifugation at 350 g for 10 min the pellet was suspended in 20 mL RPMI + 10% human serum and seeded in a T75 culture flask. To induce differentiation, either 100 ng/mL recombinant human granulocyte-macrophage colony-stimulating factor (rhuGM-CSF) or 10 ng/mL recombinant human macrophage colony-stimulating factor (rhuM-CSF) was added to the flask. The cells were then incubated at 37 °C with 5% CO_2 at 95% humidity. After three days the medium was changed, again containing the corresponding growth factor. Further three days later the cells could be seeded in preparation of the infection assay. [56]

2.2.2.2 Murine monocyte derived macrophages (mMDM)

2.2.2.2.1 Isolation of monocytes

The isolation of murine monocytes was performed by other members of the institute. For isolation of murine monocytes at first the mouse was killed by cervical dislocation. After disinfection of the skin with 70% ethanol, the hip was dislocated, and femur and tibia were isolated then separated. To sterilize the bones, they were put in 70% ethanol for 10 min and afterwards transferred to PBS-buffer for 5 min to remove remaining EtOH. The epiphysis of all bones was cut off and the marrow could be flushed into a centrifuge tube using 5 mL PBS per bone and a 20 mL syringe with a 23G needle. After one washing step with 10 mL PBS the cells were centrifuged for 10 min at 300 g. The remaining pellet was suspended in 10 mL ACK lysis buffer and centrifuged again for 10 min at 300 g. After this the cell pellet was suspended in 5.5 mL of 10% DMSO in 10% FBS solution. Aliquoted by 1.8 mL into cryotubes, the cell suspension was then slowly frozen, using a Mr. Frosty freezing container, for 24 h at -80 °C. The isolated monocytes were stored in liquid nitrogen.

2.2.2.2.2 Differentiation to murine macrophages

To differentiate the murine monocytes to murine monocyte derived macrophages (mMDMs), the isolated murine monocytes were thawed in a 37 °C water bath and washed with 10 mL of RPMI + 10% FBS. After centrifuging at 350 g for 10 min, the pellet was suspended and transferred to a T75 culture flask with 20 mL RPMI 1640 containing 10% FBS and 10 ng/mL recombinant murine macrophage colony-stimulating factor (rmM-CSF) as well as 50 µM 2-mercaptoethanol. The cells were then incubated at 37 °C with 5% CO_2 and 95% humidity and the medium was changed on the fourth day. After another four days of incubation the cells were seeded.

2.2.2.3 Cultivation of A549 cells

A549 cells were thawed in a 37 °C water bath, while 20 mL of F-12K medium with 10 % FBS were prepared in a T75 culture flask. The thawed cells were transferred to the culture flask and incubated at 37 °C with 5% CO_2 and 95% humidity. The media was changed the next day. After further five days the A549 cells were ready for seeding.

2.2.2.4 Harvest and seeding of hMDMs, mMDMs and A549 cells

In preparation of an infection assay hMDMs, mMDMs or A549 cells were harvested and seeded according to the same procedure. Firstly, the cells were washed with 7 mL PBS + 1 mM EDTA. Then 1 mL of 0,25% Trypsin/EDTA was added and incubated at 37 °C with 5% CO_2 and 95% humidity for 5 (A549) or 10 (macrophages) min. The Trypsin/EDTA was then inactivated by adding 10 mL of the corresponding medium before centrifuging at 300 g for 10 min. The pellet was then suspended in 2 (macrophages) or 10 (A549) mL medium and the cell concentration was determined. Afterwards the cells could be diluted and equally distributed onto the 48-well plate with 400 µL suspension per well. The desired concentrations were 3.25×10^5 cells/mL for the hMDMs and the mMDMs and 3.75×10^5 cells/mL for the A549 cells.

2.2.2.5 THP1 cells

2.2.2.5.1 Cultivation of THP1 cells

The THP1 and THP1-*defCasp1* cells were thawed in a 37 °C water bath and washed with 10 mL RPMI 1640 containing 10% FBS. The suspension was then centrifuged at 350 g for 10 min and the pellet suspended in 1 mL RPMI 1640 + 10% FBS. The cell concentration was determined and afterwards diluted to 5x105 cells/mL. For both cell lines 100 µg/mL Normocin was added and for the THP1-*defCasp1* cells additionally 200 µg/mL Hygromycin B Gold was added. The suspension was then transferred to T75 culture flasks (20 mL per flask) and cultured at 37 °C with 5% CO_2 and 95% humidity for three to four days. Thereafter cells could be centrifuged and suspended in 10 mL RPMI +10% FBS for either passaging or seeding and differentiation.

2.2.2.5.2 Differentiation and seeding of THP1 cells

In accordance with the protocol, THP1 cells were seeded first for infection and differentiated when seeded. Therefore, the cultured cells were centrifuged for 10 min at 300 g and the pellet suspended in RPMI + 10% FBS. The cell concentration was determined and diluted to proper cell concentration for the infection assay. For a 48-well plate each well contained 400 µL cell suspension with a concentration of $7.5x10^5$ cells/mL for THP1 cells and $8.25x10^5$ cells/mL for THP1-*defCasp1* cells. The cells were incubated for 24 h at 37 °C with 5% CO_2 and 95% humidity before adding 175 ng/mL PMA to stimulate differentiation. After further two days of incubation the medium was changed to RPMI + 10% FBS without PMA. The infection could then be performed three days afterwards. For infection however, the cell count had to be determined first, to adjust bacteria for a desired MOI. Therefore, two wells were washed with PBS + 1 mM EDTA and then incubated with 40 µL of 0.25% Trypsin/EDTA at 37 °C with 5% CO_2 at 95% humidity for 10 min. Thereafter 400 µL of RPMI medium were added to inactivate the Trypsin/EDTA and cells were detached from the well. The cell count was determined using the Luna-FX7 fluorescence cell counter.

2.2.3 Biochemical methods

2.2.3.1 Cytotoxicity assay

For determination of cell lysis, the lactate dehydrogenase, released at the loss of cell membrane integrity, was quantified. Therefore, a LDH assay was performed, using the CytoTox-One homogenous membrane integrity assay (Promega, Austria). For the assay, 50 µL of the post-infection supernatant was mixed with 50 µL of the substrate provided by the kit and incubated for 10 min in darkness. Afterwards 25 µL stop-solution were added before measuring the emission at 610 nm at an excitation of 560 nm using the microplate reader Infinite M200 PRO (Tecan, Crailsheim, Germany) [98]. To calculate a ratio, the infected samples were normalized to their corresponding not infected samples, set to 1.

2.2.4 Molecular biological methods

2.2.4.1 DNA isolation

DNA isolation from bacteria was performed using the DNA isolation kit by Macherey-Nagel according to the protocol provided by the manufacturer. The bacteria were grown overnight on an agar plate and one colony was picked on the next day for isolation of the DNA.

2.2.4.2 Verification of the *exoU* gene in *P. aeruginosa* CF1013 via PCR

To verify the presence of the *exoU* gene in the clinical *P. aeruginosa* CF1013 strain, a polymerase chain reaction was performed. Therefore, the DNA was isolated as described before and amplified using the Q5® High Fidelity DNA-Polymerase by New England Biolabs as well as the belonging Q5® Reaction buffer and Q5® High GC Enhancer. The used primers are ExoU_fw and ExoU_rv as described in the Materials chapter. After addition of nuclease-free water and dNTPs the PCR was performed using the program in Table 12 [97]. As a positive control, the plasmid from *E. coli* DHB5α (pET15b/ExoU) was used, the negative control contained PCR-water instead of a DNA template. For extraction of the *exoU* containing plasmid, the lab-intern protocol was used. The bacteria were grown overnight on an agar plate containing the indicated antibiotic. On the next day, three colonies were picked from the plate and suspended in 100 µL PCR water in a 1.5 mL reaction tube. The

suspension was then heated to 99 °C for 15 min. Afterwards it was centrifuged for 1 min at maximum rpm and the supernatant was frozen.

Table 12: PCR-program for the amplification of a part of the *exoU* gene.

Step	Temperature	Duration	Cycles
Initial Denaturation	94 °C	10 min	1
Cycle Denaturation	94 °C	30 sec	30
Cycle Annealing	Gradient (56, 58, 60, 62, 66 °C)	45 sec	
Cycle Elongation	72 °C	45 sec	
Final Elongation	72 °C	10 min	1

After the PCR, 5 µL of each sample were mixed with 1 µL 6x DNA Ladder (100 bp) and applied on an 1.5% agarose gel containing 3 µL / 100 mL Midori Green Advance. To disperse the fragments, 80 V were applied for 35 min.

Furthermore, two samples were prepared for sequencing by using the Wizard® SV Gel and PCR Clean-Up System (Promega) and the NightXpress Mix2Seq Kit (Eurofins) and sent to Eurofins for Sanger Sequencing.

2.2.5 Statistical analysis

For statistics and graphing of data, IBM SPSS Statistics 29 software was used. When comparing different conditions such as different inhibitors to a reference or infected to not-infected, an unpaired t-test was used. For comparing samples of the same condition but different time points, a paired t-test was performed. The evaluation of LDH-release in THP1 cells was performed by three biological replicates, while in the case of hMDMs two or three different donors were used.

3. Results

3.1 Establishing an infection model for detecting *P. aeruginosa* induced cell death

To examine a possible influence of the inhibition of eukaryotic lipases on non-apoptotic cell death, first lytic cell death induction was evaluated in different eukaryotic cell models.

3.1.1 Verification of the *exoU* gene on the genome of *P. aeruginosa* CF1013

To investigate the induced cell lysis, which is enhanced by ExoU, it was necessary to use an *exoU* expressing isolate. The clinical sample of *P. aeruginosa* CF1013 has been shown to express the Exotoxin U on the protein level previously (unpublished data, Dr. G. Zarfel, Diagnostic and Research Institute for Hygiene, Microbiology and Environmental Medicine, Medical University of Graz). To confirm that the *exoU* gene is encoded on the genome of the here investigated isolate, a PCR was performed. Using a plasmid that possesses the *exoU* gene, carried by a *E. coli* DHB5α as a positive control, presence of *exoU* on the *P. aeruginosa* CF1013 genome could be proven. The corresponding agarose gel is shown in Figure 2.

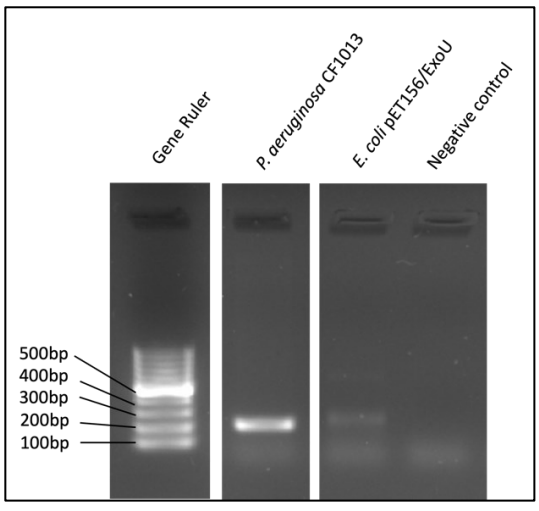

Figure 2: **Agarose gel after the performance of a PCR, using primers for a fragment of the *exoU* gene.** On the far-left the gene ruler was applied, indicating bands with 100 bp to 500 bp in 100 bp steps. On the second column the sample of genomic DNA from *P. aeruginosa* CF1013 was applied. The third column shows the positive control using a plasmid that carries the *exoU* gene. The far-right column shows the negative control using PCR-water.

The samples in Figure 2 in the second and third column refer to the sample of *P. aeruginosa* CF1013 and the positive control from the plasmid, respectively. Both samples show a band at around 200 bp. The expected bp length of the examined fragment of *exoU* is 204 bp.

3.1.2 *P. aeruginosa* CF1013 does not induce lysis in primary human macrophages

To test the possible *P. aeruginosa* dependent induction of cell lysis in human macrophages, monocytes were differentiated using rhuGM-CSF. The macrophages were then infected with different MOIs of *P. aeruginosa* and the LDH-release was measured after 0 h and 2 h. The LDH-release after 2 h of the infected relative to the not infected macrophages is displayed in Figure 3. MOI of 1n means that the infection medium was left on the cells until removing it as a supernatant.

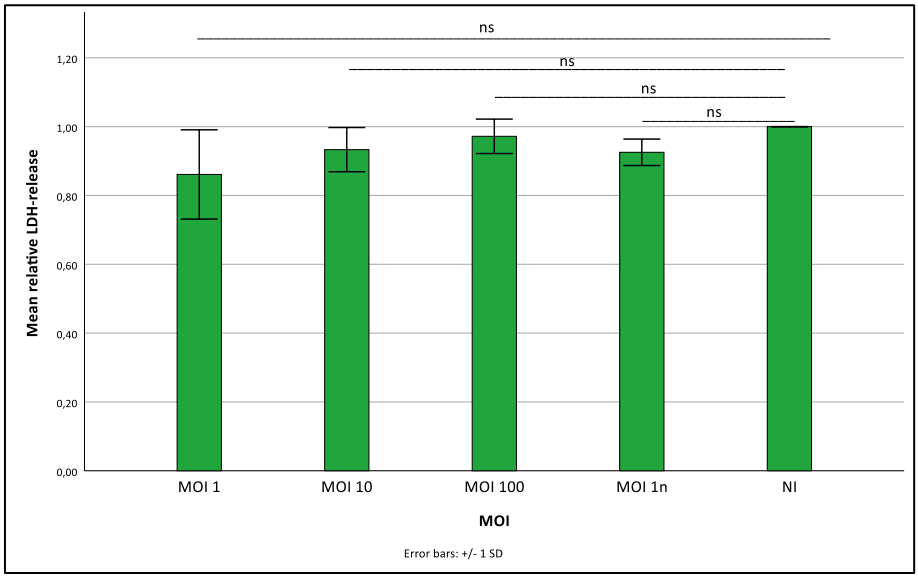

Figure 3: **Relative LDH-release of GM-CSF differentiated macrophages infected with *P. aeruginosa*.** The columns show the LDH-release of cells infected with different MOIs (1, 10, 100 and 1n (infection mix left on the cells and used as the supernatant)) normalized to a not infected control (NI, set to 1), all labelled at the x-axis. The columns show the mean, and the error bars mark the standard deviation. The experiment was performed in three biological replicates and three technical replicates each. Significance was tested via unpaired t-tests.

No significant difference was observed between the infected samples and the not infected control, indicating that *P. aeruginosa* CF1013 does not induce cell lysis in GM-CSF differentiated human macrophages.

The mean extracellular bacterial load in CFU/mL of the different MOIs at different time points are depicted in Figure 4.

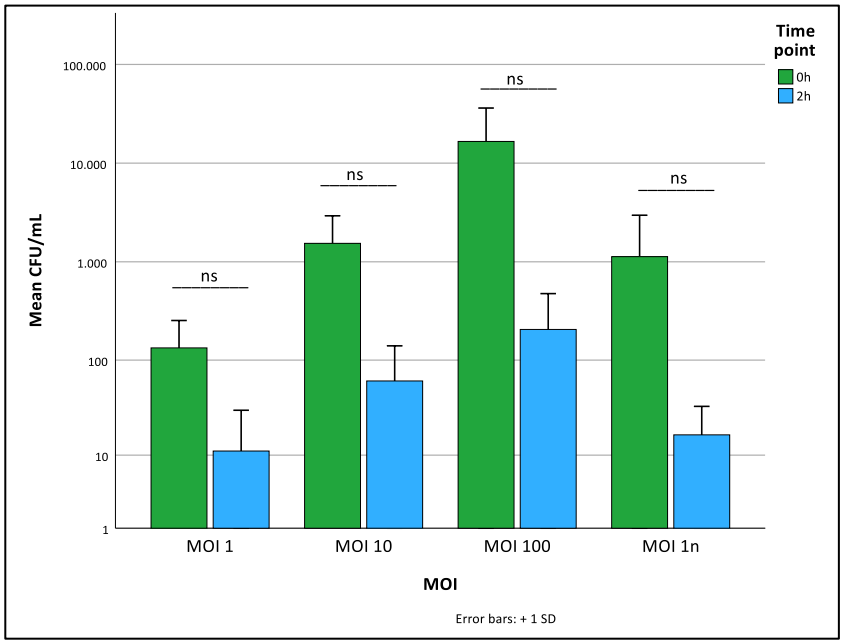

Figure 4: **CFU/mL of *P. aeruginosa* in the supernatant after 0 h and 2 h of infection.** The infected cells were human monocytes differentiated to macrophages by GM-CSF. The green columns show the value of the 0 h sample, the blue columns show the value of the 2 h sample. The used MOIs (1, 10, 100 and 1n (infection mix left on the cells and used as the supernatant)) are labelled on the x-axis, while the y-axis shows the CFU/mL. The experiment was performed three times, i.e. the columns show the mean of three biological replicates, each consisting of three technical replicates, while the error bars depict the standard deviation. Due to the logarithmic scale, the error bars of the standard deviation are only shown in the positive direction. Significance was tested via paired t-tests.

Figure 4 shows a decrease of *P. aeruginosa* in the cells infected with MOI 1 and 10 in CFU/mL extracellular bacterial load of about one logarithmic step, from approximately 100 to 10 in MOI 1 and 1,000 to 100 in MOI 10. The CFU/mL in cells infected with MOI 100 and 1n shows a decrease of about two logarithmic steps. In cells infected with MOI 100 the CFU/mL decreases from approximately 10,000 to 100 and MOI 1n from 1,000 to 10. However, paired t-tests show that none of these changes in CFU/mL are significant (*p*-values between 0.093 and 0.201), which needs to be investigated in additional experiments.

In a subsequent assay the macrophages were differentiated by rhuM-CSF, another colony stimulating factor. This factor has been used by Bagayoko *et. al* [20], where they showed cell lysis induced by another strain of *P. aeruginosa* (PP34 *exoU*$^{+}$) in these cells. Additionally, the T3SS in *P. aeruginosa* was induced, adding EGTA to its culture, since ExoU is secreted via this system [19]. EGTA is a chelator binding particularly Ca2+-ions which leads to Ca2+ limited growth that has been shown to induce T3SS expression [99]. The LDH-release after 2 h of the infected relative to the not infected macrophages is displayed in Figure 5.

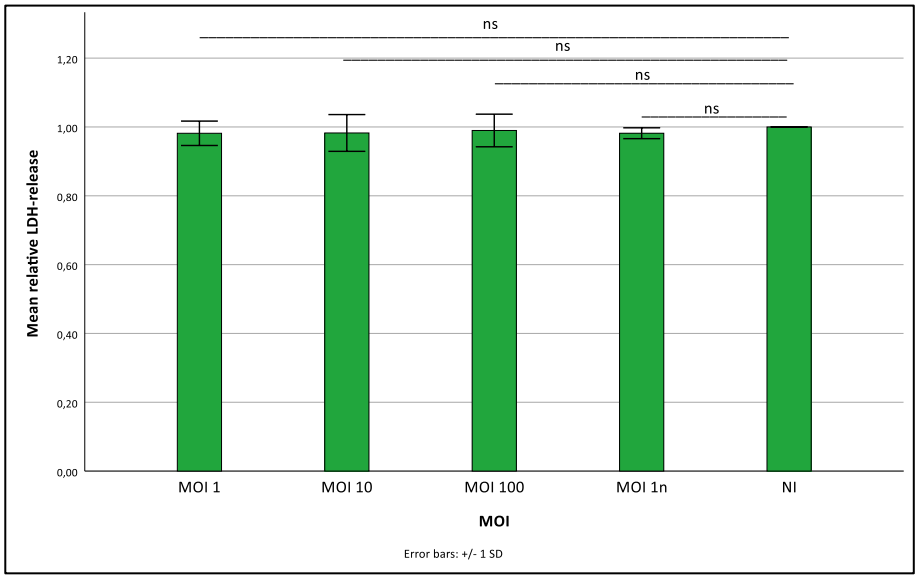

Figure 5: **Relative LDH-release of M-CSF differentiated macrophages infected with *P. aeruginosa*.** The columns show the LDH-release of cells infected with different MOIs (1, 10, 100 and 1n (infection mix left on the cells and used as the supernatant)), normalized to a not infected control (NI, set to 1), all labelled at the x-axis. The columns show the mean, and the error bars mark the standard deviation. The experiment was performed in three biological replicates and three technical replicates each. Significance was tested via unpaired t-tests.

Figure 5 shows that no significant difference between the infected cells and the control was observed.

For this experiment the mean CFU/mL of extracellular bacterial load was also examined and visualized in Figure 6.

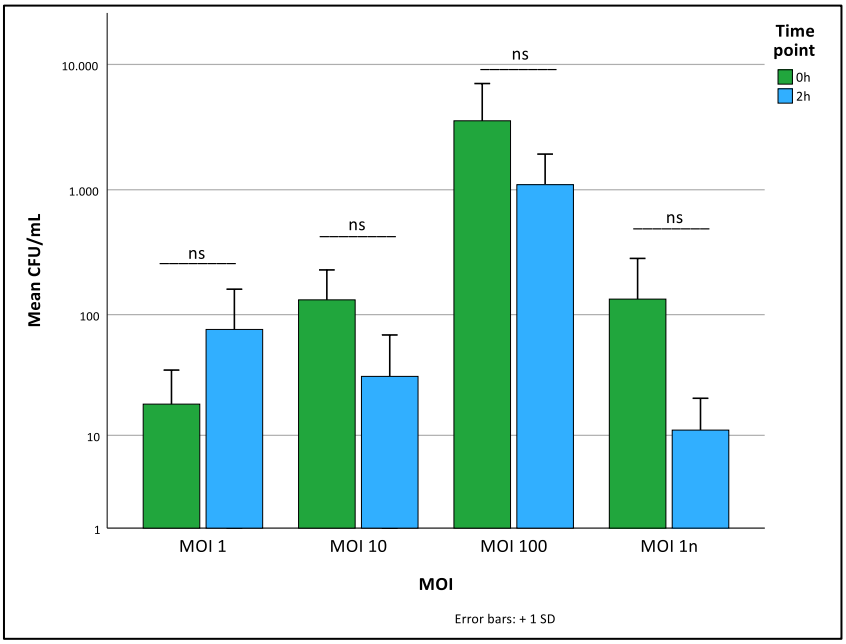

Figure 6: **CFU/mL of *P. aeruginosa* in the supernatant after 0 h and 2 h of infection.** The infected cells were human monocytes differentiated to macrophages by M-CSF. The green columns show the value of the 0 h sample, the blue columns show the value of the 2 h sample. The used MOIs (1, 10, 100 and 1n (infection mix left on the cells and used as the supernatant)) are labelled on the x-axis, while the y-axis shows the CFU/mL. The experiment was performed three times, i.e. the columns show the mean of three biological replicates, each consisting of three technical replicates, while the error bars depict the standard deviation. Due to the logarithmic scale, the error bars of the standard deviation are only shown in the positive direction. Significance was tested via paired t-tests.

The experiment showed no significant changes in CFU/mL of extracellular bacterial load between the time points (*p*-values between 0.115 and 0.162) Nevertheless, Figure 6 shows some tendencies. The CFU/mL in cells infected with MOI 1 increases from 0 h to 2 h by about the half of a logarithmic step (approximately 18 to 75). Meanwhile the other tested MOIs show a decrease in CFU/mL over time. MOI 100 decreases half a logarithmic step (3,500 to 1,000), while MOI 10 and 1n both decrease about one logarithmic step (130 to 30 or 10, respectively).

3.1.3 *P. aeruginosa* CF1013 does not induce cell lysis in murine macrophages

To determine whether *P. aeruginosa* induces cell death in murine macrophages, murine monocytes were differentiated with rmM-CSF. The macrophages were infected with different MOIs, specifically MOI 1, 10, 100 and 1n, which meant that the infection mix was left on the cells until removing it as a supernatant. The *P. aeruginosa* sample was again cultured with the addition of EGTA to induce T3SS expression. The LDH-release after 2 h of the infected relative to the not infected macrophages is visualized in Figure 7.

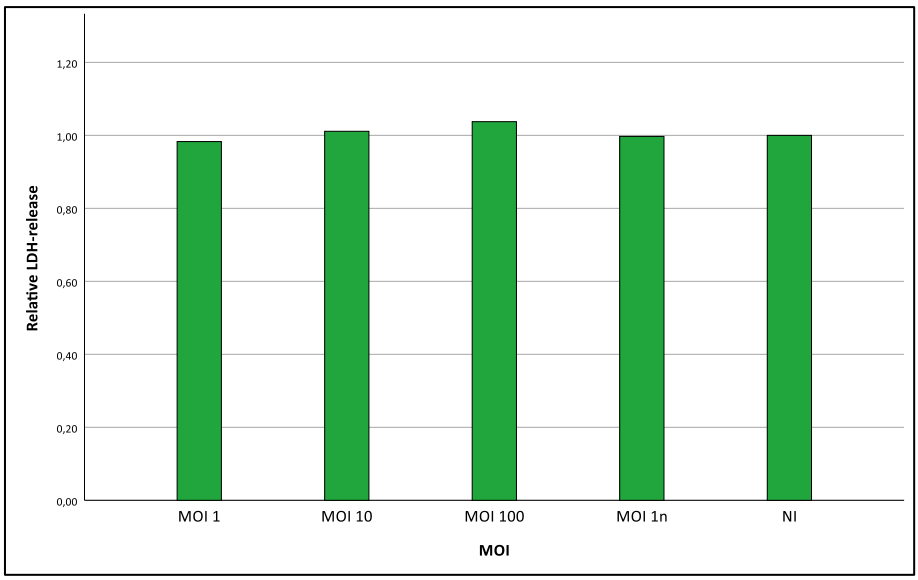

Figure 7: **Relative LDH-release of M-CSF differentiated murine macrophages infected with *P. aeruginosa*.** The columns show the LDH-release of cells infected with different MOIs (1, 10, 100 and 1n (infection mix left on the cells and used as the supernatant)) normalized to a not infected control (NI, set to 1), all labelled at the x-axis. This experiment was performed once, the columns show one biological replicate, performed in three technical replicates.

Figure 7 shows that in this experiment, there is no observable difference between the infected and not infected group. Since this experiment was only performed once, no significance could be tested.

As for the human macrophages in 3.1.2, the CFU/mL of extracellular bacterial load at the 0 h and 2 h time point was also determined for the murine macrophage experiment. The values of those measurements are depicted in Figure 8.

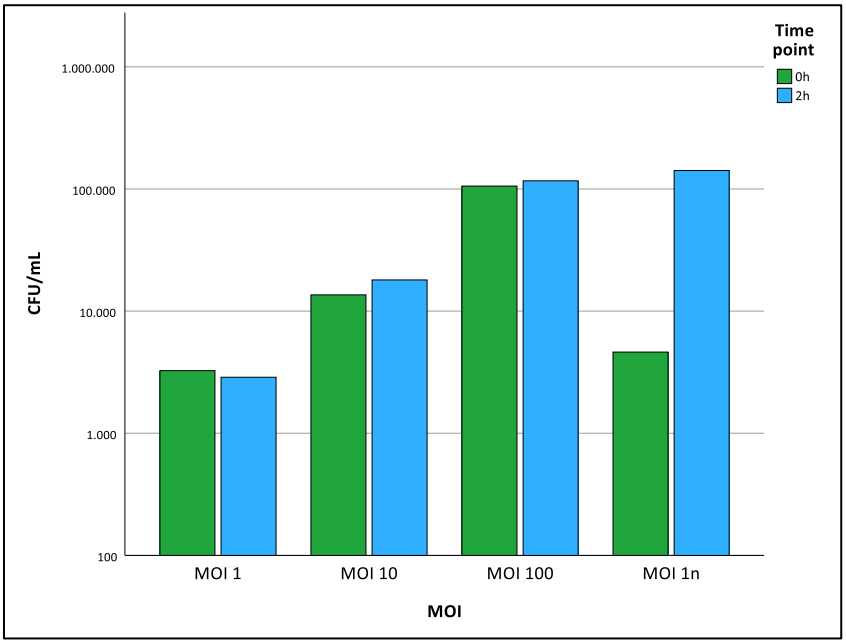

***Figure 8:* CFU/mL of *P. aeruginosa* in the supernatant after 0 h and 2 h of infection.** The infected cells were murine monocytes differentiated to macrophages by M-CSF. The green columns show the value of the 0 h sample, the blue columns show the value of the 2 h sample. The used MOIs (1, 10, 100 and 1n (infection mix left on the cells and used as the supernatant) are labelled on the x-axis, while the y- axis shows the CFU/mL. The experiment was performed once, i.e. one biological replicate, consisting of three technical replicates.

In the graph in Figure 8 it is visible that in cells infected with MOI 1 of *P. aeruginosa*, the CFU/mL of extracellular bacterial load drops slightly for 0 h to 2 h (3,200-2,900). MOI 10 and 100 both show a minor increase in CFU/mL (13,500-18,000 and 105,000-115,000), while MOI 1n shows the largest increase of about 1.5 logarithmic steps (4,500-140,000). Since this experiment was only performed once, no significance could be tested.

3.1.4 *P. aeruginosa* CF1013, *E. coli* (pET15b/ExoU) and *B. thailandensis* do not induce substantial lysis in A549 cells

To test, whether the *P. aeruginosa* strain induces cell lysis in other cells than human or murine macrophages, cells from the A549 cell line, epithelial lung cancer cells [92], were infected as well. At first, only *P. aeruginosa* was used in the same MOIs as previously (1, 10, 100 and 1n (infection mix left on the cells and used as the supernatant)). The relative LDH-release to not infected cells after 2 h for this experiment is displayed in Figure 9.

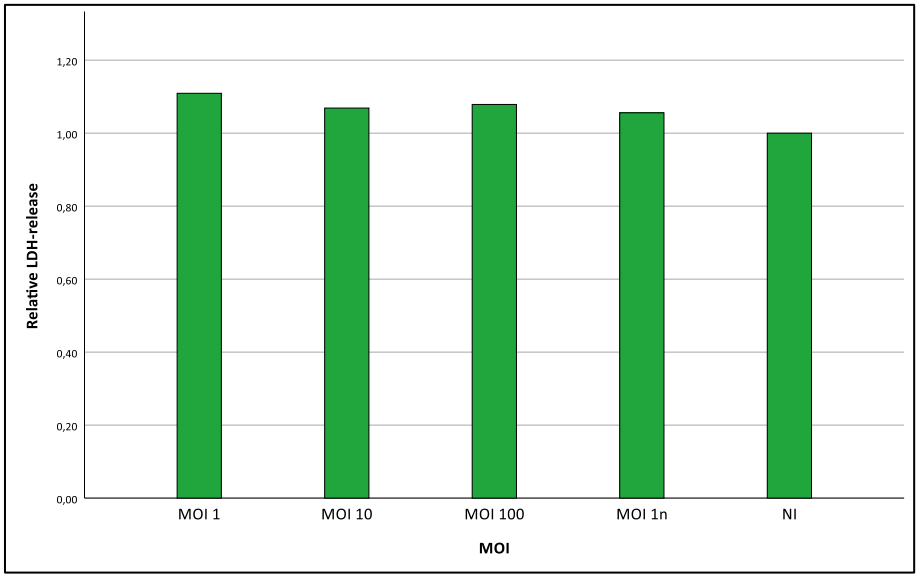

Figure 9: **Relative LDH-release of A549 cells infected with *P. aeruginosa*.** The columns show the LDH-release of cells infected by different MOIs (1, 10, 100 and 1n (infection mix left on the cells and used as the supernatant)) normalized to a not infected control (NI, set to 1), all labelled at the x-axis. This experiment was performed once, the columns show one biological replicate, consisting of three technical replicates.

In Figure 9 all infected samples show a slightly higher LDH-release than the not infected control. Since this experiment was only performed once, no significance could be tested.

Subsequently, A549 cells were infected with *P. aeruginosa*, as well as *B. thailandensis* and *E. coli* (pET15b/ExoU). *B. thailandensis* secretes ExoU as well, using the T3SS, and *E. coli* (pET15b/ExoU) carries a plasmid that expresses *exoU. P. aeruginosa* was cultured with addition of EGTA to induce the T3SS expression. Those three bacterial strains were then used to infect A549 cells with a MOI of 100 and again, the relative LDH-release to not infected cells was measured after 2 h and is displayed in Figure 10.

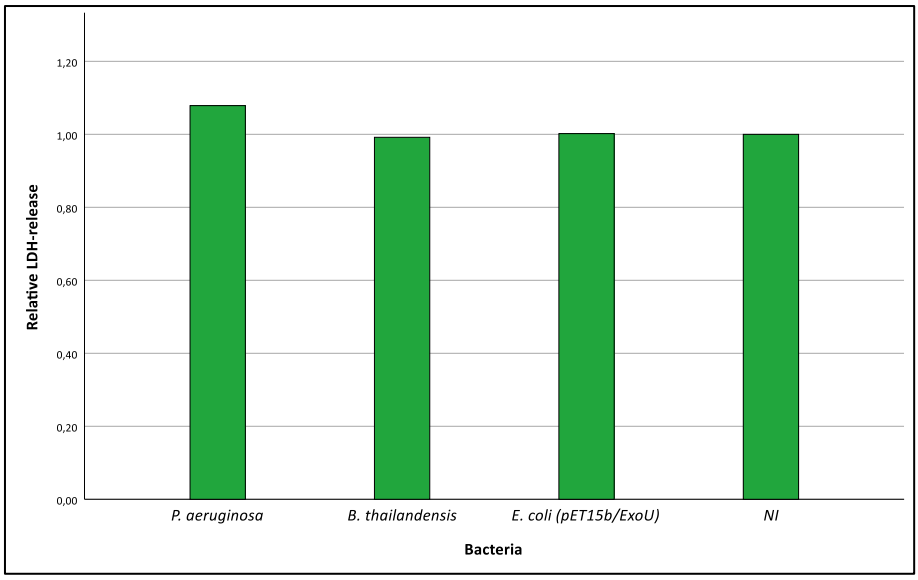

Figure 10: **Relative LDH-release of A549 cells infected with *P. aeruginosa*, *B. thailandensis* or *E. coli*.** The columns show the LDH-release of cells infected by the three different bacterial species, at a MOI of 100, relative to a not infected control (NI, set to 1), all labelled at the x-axis. This experiment was performed once, the columns show one biological replicate, consisting of three technical replicates.

In Figure 10, although *P. aeruginosa* shows a higher value of relative LDH-release that the other bacteria (1.079), none showed a notably visible difference compared to the not infected control. Since this experiment was only performed once, no significance could be tested.

The CFU/mL of extracellular bacterial load at the 0 h and 2 h time point was also determined. The corresponding values for the experiment of different MOIs with *P. aeruginosa* are visualized in Figure 11.

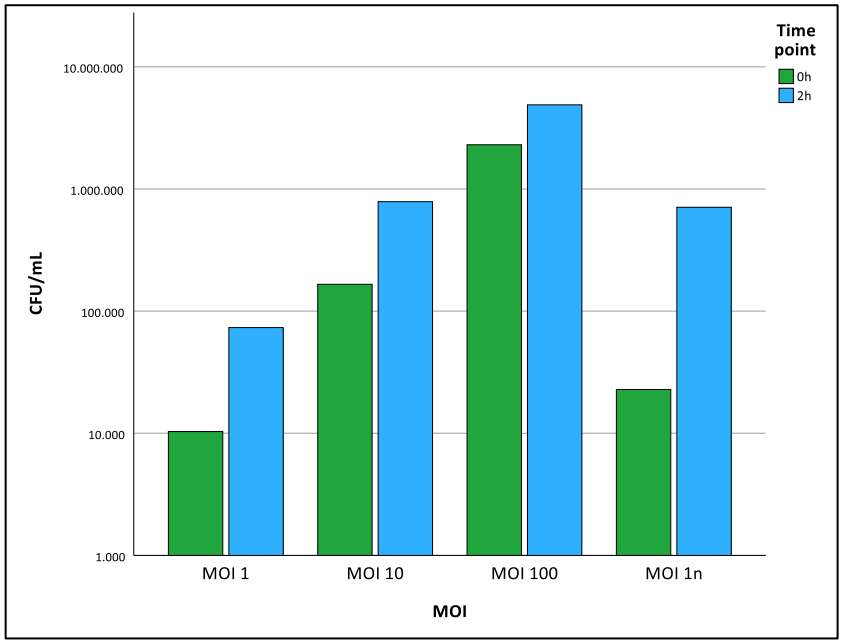

***Figure 11:* CFU/mL of *P. aeruginosa* in the supernatant after 0 h and 2 h of infection.** The infected cells were A549 cells. The green columns show the value of the 0 h sample, the blue columns show the value of the 2 h sample. The used MOIs (1, 10, 100 and 1n (infection mix left on the cells and used as the supernatant)) are labelled on the x-axis, while the y-axis shows the CFU/mL. The experiment was performed once, i.e. one biological replicate, consisting of three technical replicates.

Figure 11 shows an increase in the CFU/mL in all four different MOIs used over time. Hereby the factor of increase varies between the different MOIs with cells infected with MOI 1n showing the largest margin in the logarithmic graph. Since this experiment was only performed once, no significance could be tested.

For the experiment with the bacteria *P. aeruginosa*, *B. thailandensis* and *E. coli*, the CFU/mL values at the time points 0 h and 2 h are depicted in Figure 12.

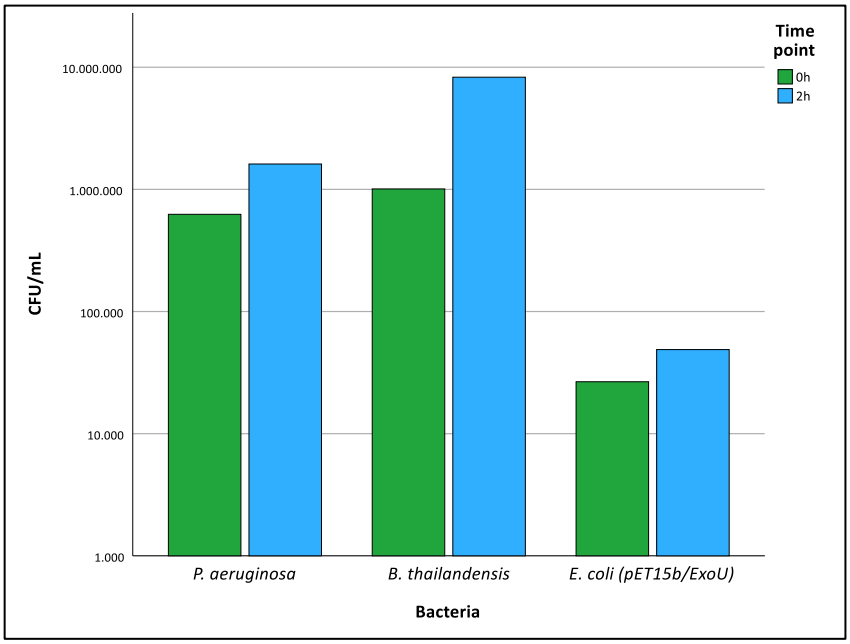

Figure 12: **CFU/mL of *P. aeruginosa*, *B. thailandensis* and *E. coli* in the supernatant after 0 h and 2 h of infection.** The infected cells were A549 cells. The green columns show the value of the 0 h sample, the blue columns show the value of the 2 h sample. The used bacteria are labelled on the x-axis, while the y-axis shows the CFU/mL. The experiment was performed once, i.e. one biological replicate, consisting of three technical replicates.

In Figure 12, the columns of all used bacteria again show an increase from 0 h to 2 h. Although all bacteria were used at a MOI of 100, *E. coli* stands out, showing an overall lower CFU/mL in extracellular bacterial load at 0 h as well as at 2 h. Since this experiment was only performed once, no significance could be tested.

3.1.5 *P. aeruginosa* CF1013, *E. coli* (pET15b/ExoU) and *B. thailandensis* induce cell lysis in THP1-*null* cells

The next cells that were tested for cell lysis after infection, were THP1 cells, a cell line of monocytic cells, obtained from an acute leukemia patient [94]. Like the A549 cells in 3.1.4, the THP1-*null* cells were first infected with *P. aeruginosa*. Then the relative LDH-release was measured after 2 h, displayed in Figure 13.

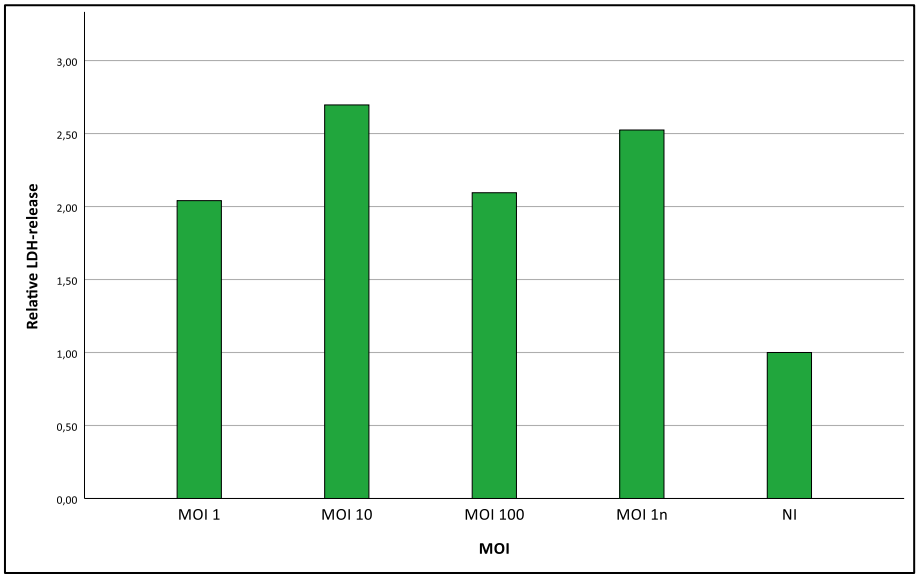

Figure 13: **Relative LDH-release of THP1-*null* cells infected with *P. aeruginosa*.** The columns show the LDH-release of cells infected by different MOIs (1, 10, 100 and 1n (infection mix left on the cells and used as the supernatant)), normalized to a not infected control (NI, set to 1), all labelled at the x-axis. This experiment was performed once, the columns show one biological replicate, consisting of three technical replicates.

Figure 13 shows that all infected samples show more than twice the signal in LDH-release compared to the not infected control. Interestingly there is no visible correlation between the amount of LDH-release and the MOI; cells infected with MOI 10 showing the highest value with 2.696 times the signal in LDH-release as not infected. The lowest infected value is shown by cells infected with MOI 1 at 2.040. Since this experiment was only performed once, no significance could be tested.

Afterwards the experiment was repeated with *B. thailandensis* and *E. coli* (pET15b/ExoU), using MOI 100. The respective LDH-release compared to a not infected control, as well as the LDH-release of *P. aeruginosa* at MOI 100 after 2 h is visible in Figure 14.

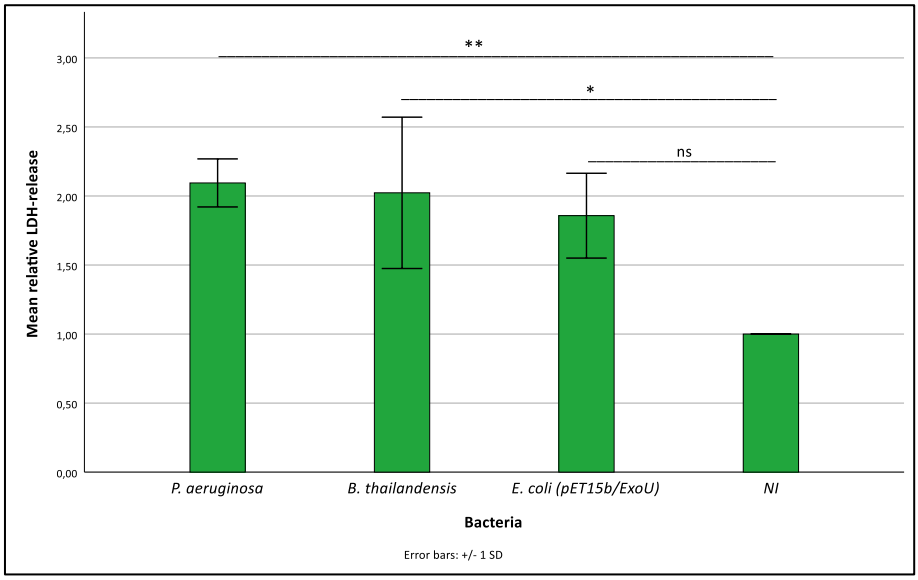

Figure 14: **Relative LDH-release of THP1-*null* cells infected with *P. aeruginosa*, *B. thailandensis* or *E. coli*.** The columns show the LDH-release of cells infected by the three different bacterial species, at a MOI of 100, normalized to a not infected control (NI, set to 1), all labelled at the x-axis. The experiment was performed twice in three technical replicates each. The columns display the mean of the biological replicates while the error bars show the standard deviation. Significance was tested via unpaired t-tests.

Figure 14 shows the highest value of LDH-release in cells infected with *P. aeruginosa* with 2.094 (± 0.174), while cells infected with *E. coli* show the lowest value of the infected samples, that is 1.858 (± 0.307). Although there are only two biological replicates, t-tests were performed between the infected samples compared to the not infected control. *P. aeruginosa* and *E. coli* show significant differences to the not infected control ($p = 0.006$ for *P. aeruginosa* and $p = 0.029$ for *E. coli*). *B. thailandensis* does not show a significant difference to the not infected control but is still very close to a significant *p*-value ($p = 0.059$). Therefore, all three bacterial species induce cell lysis in THP1 cells. However, these results need to be confirmed by additional biological replicates.

The CFU/mL of extracellular bacterial load was determined as previously. The sample values for the different MOIs of *P. aeruginosa* are visualized in Figure 15.

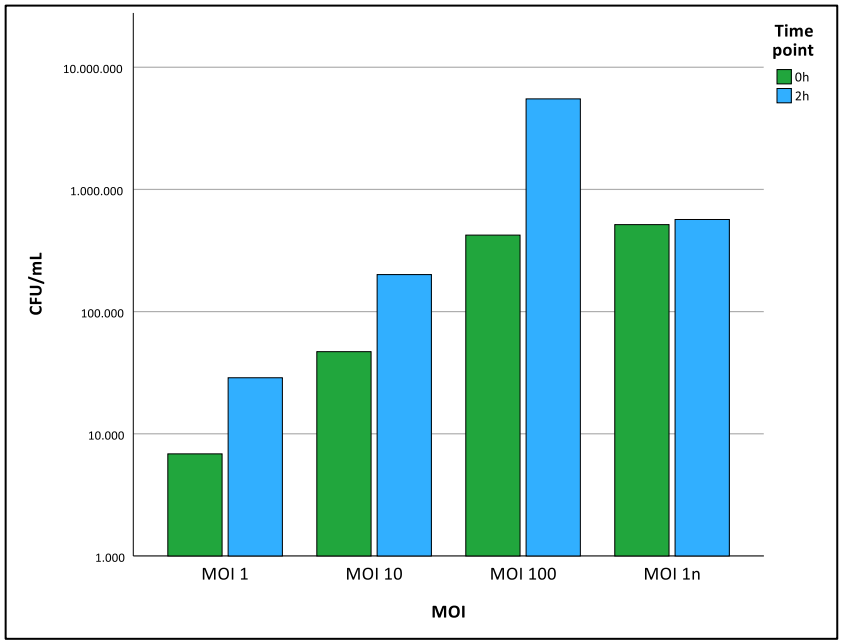

***Figure 15:* CFU/mL of *P. aeruginosa* in the supernatant after 0 h and 2 h of infection.** The infected cells were THP1-*null* cells. The green columns show the value of the 0 h sample, the blue columns show the value of the 2 h sample. The used MOIs (1, 10, 100 and 1n (infection mix left on the cells and used as the supernatant)) are labelled on the x-axis, while the y-axis shows the CFU/mL. The experiment was performed once, i.e. one biological replicate that consists of three technical replicates.

Figure 15 shows an increase in all different variants of used MOI from the 0 h to the 2 h sample, except for MOI 1n. The CFU/mL in the supernatant of cells infected with MOI 1, 10 and 100 increases from 0 h to 2 h with cells infected with MOI 100 showing the largest difference. Cells infected with MOI 1n instead show no visible increase nor decrease in CFU/mL of extracellular bacterial load from 0 h to 2 h. Since this experiment was only performed once, no significance could be tested.

The CFU/mL was determined for the experiment with three different bacteria as well. Those are visualized in Figure 16.

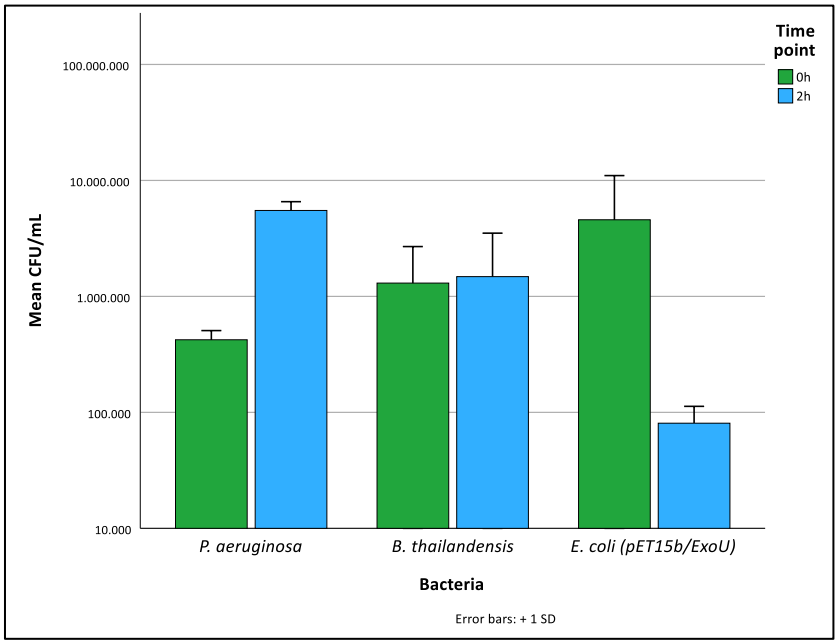

Figure 16: **CFU/mL of *P. aeruginosa*, *B. thailandensis* and *E. coli* in the supernatant after 0 h and 2 h of infection.** The infected cells were THP1-*null* cells. The green columns show the value of the 0 h sample, the blue columns show the value of the 2 h sample. The used bacteria are labelled on the x-axis, while the y-axis shows the CFU/mL. The experiment was performed twice, i.e. two biological replicates, consisting of three technical replicates each. The columns show the mean of the biological replicates while the error bars indicate the standard deviation. Due to logarithmic scale, the error bars of the standard deviation are only shown in the positive direction.

While *P. aeruginosa* shows an increase in CFU/mL in Figure 16, *B. thailandensis*, in contrast to the A549 cells, shows almost no increase nor decrease at all. *E. coli* in turn shows a rather large decrease in CFU/mL of extracellular bacterial load.

3.2 Ferrostatin-1 does not inhibit cell lysis in infected THP1-*null* cells

As a next step, it was investigated, what kind of lytic cell death *P. aeruginosa* CF1013 induces in THP1 cells. Therefore, THP1-*null* cells were again infected with *P. aeruginosa*, *B. thailandensis* and *E. coli* and treated with ferrostatin-1. Ferrostatin-1 is described to inhibit ferroptosis, one possible kind of cell death, that is described to be triggered by *P. aeruginosa* and fueled by ExoU [20, 47]. The LDH-release after 2 h is shown in Figure 17.

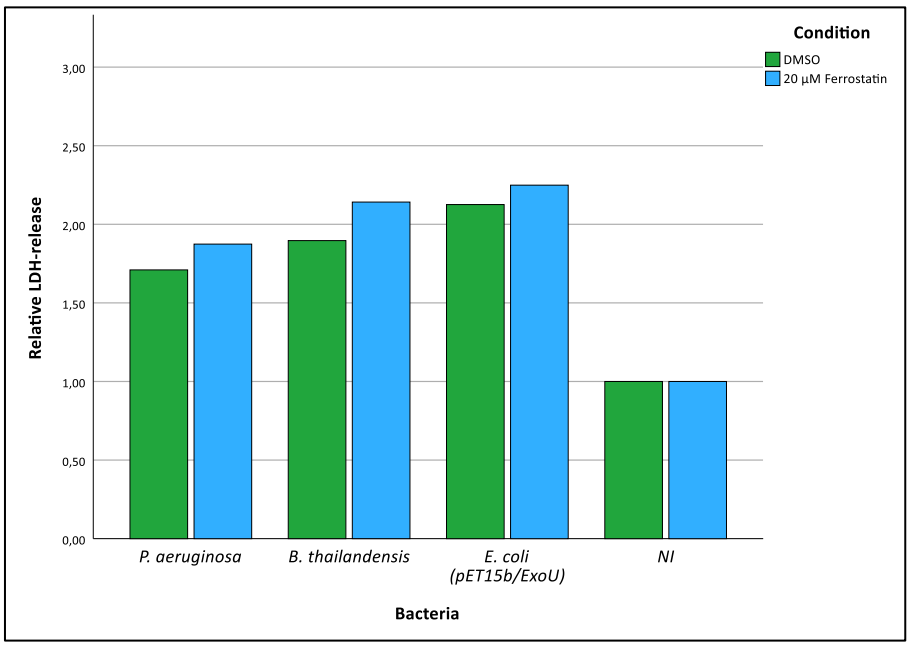

Figure 17: **Relative LDH-release of THP1-*null* cells infected with *P. aeruginosa*, *B. thailandensis* and *E. coli*.** The columns show the LDH-release of cells infected by the three different bacterial species, at a MOI of 100, normalized to a not infected control (NI, set to 1), all labelled on the x-axis. The different colours indicate the two conditions, the cells were supplemented with. Green indicates the control with DMSO, blue indicates the addition of 20 µM ferrostatin-1. This experiment was performed once, the columns show one biological replicate, consisting of three technical replicates.

As visible in Figure 17, cells infected with all bacterial species show an increased LDH-release compared to the not infected control. In all three the LDH-release with ferrostatin-1 is slightly higher than with the DMSO control. This result indicates that ferrostatin-1 does not inhibit the cell lysis and thereby suggests that the observed lytic cell death is not ferroptosis. The possibility of ferroptosis induction cannot be completely ruled out, since another cell death mechanism, such as pyroptosis, may compensate. Since this experiment was only performed once, no significance could be tested.

To examine a possible influence of DMSO or ferrostatin-1 on the bacterial load, the CFU/mL was also determined at 0 h and 2 h samples. The CFU/mL of the different bacteria is shown in Figure 18.

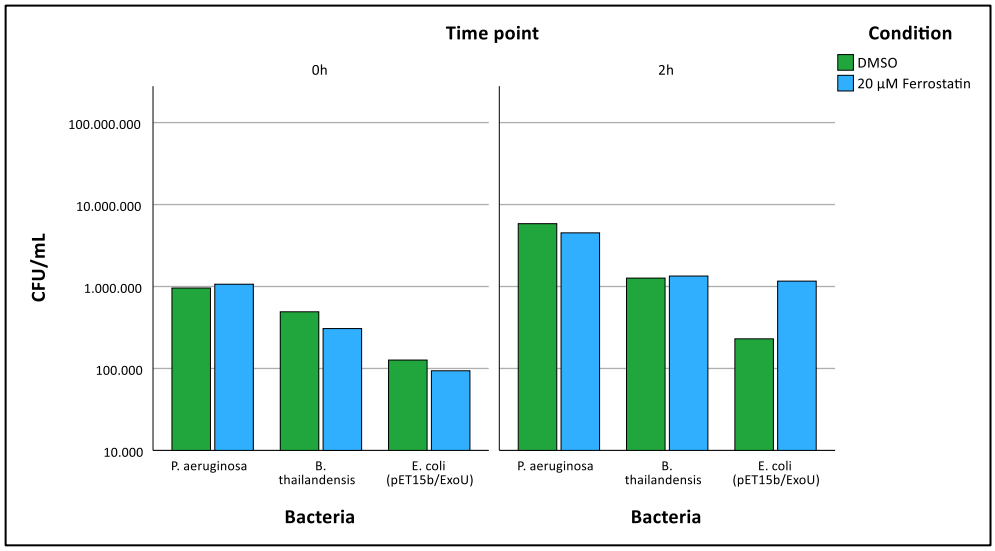

Figure 18: **CFU/mL of *P. aeruginosa*, *B. thailandensis* and *E. coli* in the supernatant after 0 h and 2 h of infection.** The infected cells were THP1-*null* cells. The green columns show the value of the DMSO treated sample, the blue columns show the value of the ferrostatin-1 treated sample. The used bacteria are labelled on the x-axis, while the y-axis shows the CFU/mL. As indicated above, the graph is also split into two sections. The left one shows the values for the 0 h samples, the right section depicts the values for the 2 h samples. This experiment was performed once, the columns show one biological replicate, consisting of three technical replicates.

The first visible fact is, although all bacteria were used for infection at the same MOI (MOI 100), they vary in the 0 h value, *E. coli* being almost a whole logarithmic step lower than *P. aeruginosa*. Meanwhile there is no visible difference between the two conditions within each time point. The only exception to this is *E. coli* after 2 h infection, showing about by the factor 10 higher values with ferrostatin-1 than in the DMSO control. Besides that, all bacteria show an increase in CFU/mL after 2 h, no matter the condition. Since this experiment was only performed once, no significance could be tested.

3.3 Influence of lipase inhibitors on *P. aeruginosa* CF1013 infected THP1-*defCasp1* cells

Since pyroptosis is a possible kind of cell death that could compensate ferroptosis in cell lysis, it was to determine whether lytic cell death could be observed when pyroptosis is reduced. This could be achieved through the genetic depletion of caspase-1.

Therefore, THP1-*defCasp1* cells were used [96]. Now the DMSO control was used, as well as ferrostatin-1, also a control using no supplement to examine a general induction of lysis in those cells. This time also different lipase inhibitors (JZL184 for MAGL, atglistatin for ATGL and KT182 for ABHD6) were used to examine a possible influence of these in pathogen-induced cell death. The relative LDH-release of infected to not infected cells after 2 h is shown in Figure 19.

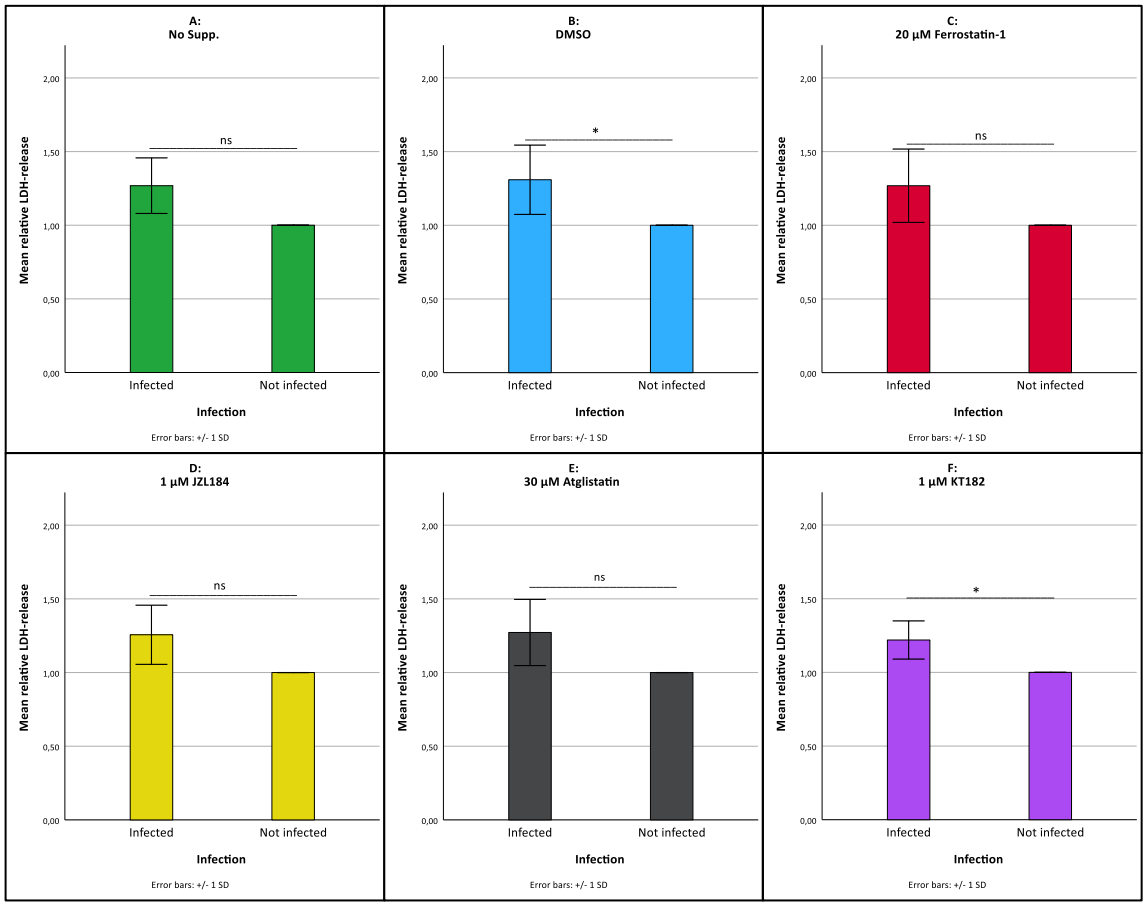

Figure 19: **Relative LDH-release of THP1-*defCasp1* cells infected with *P. aeruginosa* under different conditions.** The columns show the LDH-release of cells under the six different conditions, normalized to the respective not infected control (set to 1). **A:** No supplement added; **B:** Addition of DMSO; **C:** Addition of 20 µM ferrostatin-1; **D:** Addition of 1 µM JZL184; **E:** Addition of 30 µM atglistatin; **F:** Addition of 1 µM KT182. The columns show the mean, and the error bars mark the standard deviation. The experiment was performed in three biological replicates and three technical replicates each. Significance was tested via unpaired t-tests.

Figure 19 shows only a slight increase in LDH-release in infected cells compared to the not infected control throughout all different conditions. Applying t-tests comparing the infected to their corresponding not infected control states that only DMSO and KT182 (**B** and **F**) differ significantly in cell lysis (DMSO p = 0.043; KT182 p = 0.049), all the other (**A**, **C**-**E**) show no significant rise in LDH-release (ferrostatin-1 p = 0.101; JZL184 p = 0.079; atglistatin p = 0.085). This is interesting especially in the cells with no supplement added because it indicates that the THP1-*defCasp1* cells, in contrast to the THP1-*null* cells, show no significant lysis when infected with *P. aeruginosa* CF1013 (p = 0.066). However, the p-values of those showing no significance are low, implying that they are close to becoming significant. To confirm these results, further replicates would be needed to increase the implied significance.

To compare the infections with supplements added to the DMSO control, the LDH-release values of those cells are displayed in Figure 20. The depicted LDH-release values are the 2 h samples to their respective not infected control (not depicted).

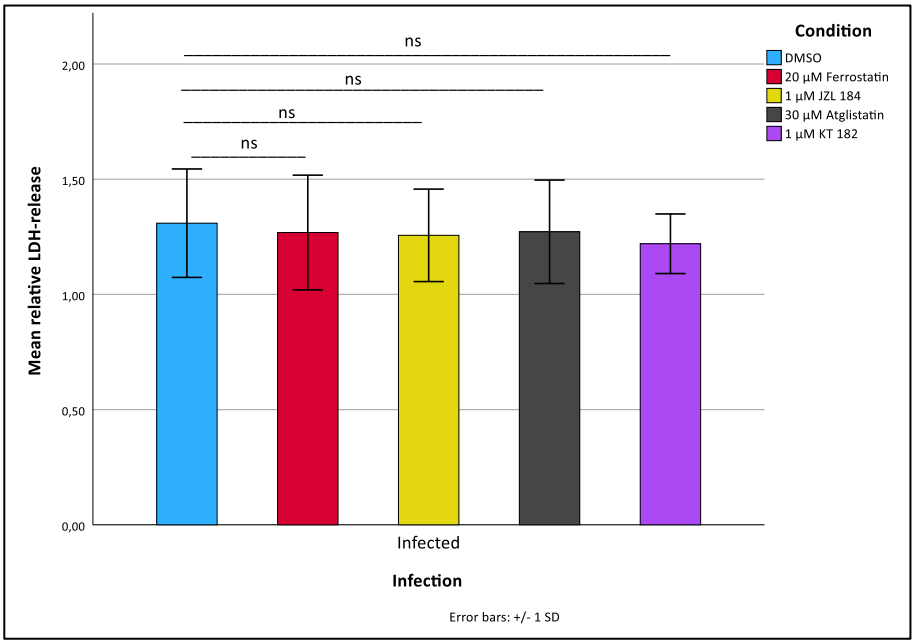

Figure 20: **Relative LDH-release of THP1-*defCasp1* cells infected with *P. aeruginosa* under different conditions.** The columns show the LDH-release of cells under the five different supplement conditions, normalized to the respective not infected control (set to 1, not depicted). Blue: Addition of DMSO; Red: Addition of 20 µM ferrostatin-1; Yellow: Addition of 1 µM JZL184; Black: Addition of 30 µM atglistatin; Violet: Addition of 1 µM KT182. The columns show the mean, and the error bars mark the standard deviation. The experiment was performed in three biological replicates and three technical replicates each. Significance was tested via unpaired t-tests.

Overall, in Figure 20 no significant difference could be observed between the control (DMSO) and any of the tested inhibitors.

As well as in other experiments, the CFU/mL of extracellular bacterial load after 0 h and 2 h was determined and the values are depicted in Figure 21.

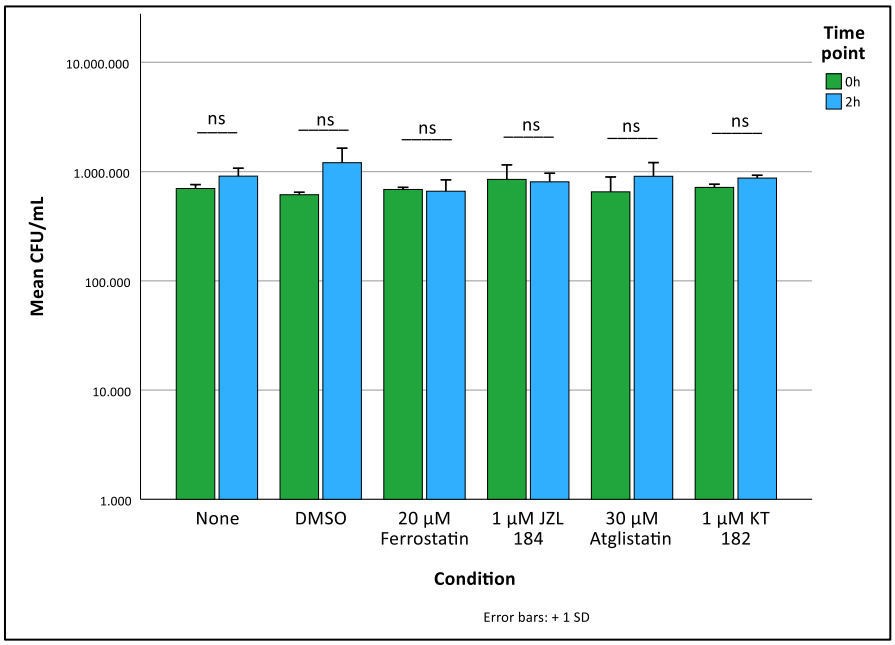

Figure 21: **CFU/mL of *P. aeruginosa* in the supernatant after 0 h and 2 h of infection.** The green columns show the value of the 0 h sample, the blue columns show the value of the 2 h sample. The different conditions that the cells were incubated with (No supplement, DMSO, 20 µM ferrostatin-1, 1 µM JZL184, 30 µM atglistatin and 1 µM KT182) are labelled on the x-axis, while the y-axis shows the CFU/mL. The experiment was performed three times, i.e. the columns show the mean of three biological replicates, each consisting of three technical replicates, while the error bars depict the standard deviation. Due to logarithmic scale, the error bars of the standard deviation are only shown in the positive direction. Significance was tested via paired t-tests.

Figure 21 shows that the lipase inhibitors as well as ferrostatin-1 and DMSO do not show a visible difference compared to the control with no supplement. None of the tested conditions show an increase nor decrease in CFU/mL from 0 h to 2 h. Neither do the controls without a supplement or DMSO. Comparing the conditions within the 0 h time point there is also no visible difference, neither is within the 2 h time point.

4. Discussion

Infection of eukaryotic cells with bacteria like *P. aeruginosa* was shown to lead to various kinds of non-apoptotic cell deaths such as ferroptosis and pyroptosis [20, 52]. It was also shown that the peroxidation of lipids like arachidonic acid and ferroptosis show close relation to each other [20]. Due to the association between peroxidized PUFAs and ferroptosis, the hypothesis of this thesis was that an inhibition of certain lipases would decrease the abundance of those PUFAs in the membrane and therefore their availability for peroxidation. Hence the consequence would be less cell lysis and an accumulation of precursors like 2-AG which exerts an anti-inflammatory effect on the cells [71, 72]. In detail it should be examined if the clinical isolate *P. aeruginosa* CF1013 induces a form of lytic cell death and if so, does the inhibition of the lipases MAGL, ATGL and ABHD6 influence the induced cell death.

4.1 *P. aeruginosa* induces lytic cell death in THP1 cells

To explore the impact of inhibiting specific eukaryotic lipases (MAGL, ATGL and ABHD6) on cell death induction, an infection model for *P. aeruginosa* CF1013 was established. After infecting various cell types with the mentioned isolate (hMDMs, mMDMs, A549 cell line, THP1 cell line), it could be shown that *P. aeruginosa* CF1013 does indeed induce cell death in THP1 cells at 2 h after infection. The results (3.1.5) show a significant increase in LDH-release, two hours after infection, not only when THP1 cells were infected with *P. aeruginosa* CF1013 but also with *B. thailandensis* and a strain of *E. coli* carrying the plasmid pET15b/ExoU. Since it was hypothesized that cell death induction is at least partially dependent on the T3SS effector ExoU, its expression was induced using EGTA when infecting THP1 cells [20, 99]. The experiment showed a significant result in lysis with two replicates. However, this must be verified by further replicates to substantiate the claimed statement.

Literature has shown significant cell death induction by an *exoU* expressing strain of *P. aeruginosa* (PP34) in murine BMDMs (bone marrow derived macrophages) and also an inhibition of that lysis by ferrostatin-1, indicating that the cell death is ferroptosis [20, 47].

Despite the adaption of the protocol in this project it could not be shown that the clinical isolate *P. aeruginosa* CF1013 although also expressing *exoU*, does not induce any kind of lysis in human MDMs or murine MDMs. The reasons for that could be various. Firstly, other factors encoded on the genome could be interfering with the induction of cell lysis and ferroptosis in macrophages. Also, despite the verification of *exoU* on the genome as well as on protein level, the concentration released could vary compared to the strain used in the previous study (Bagayoko *et. al*, 2021 [20]). Therefore, using the *exoU* expressing strain *P. aeruginosa* PP34 could be one approach to test the lysis in human and murine macrophages. Also to afterwards examine the influence of the lipase inhibitors on then possibly induced cell death as well as to test and compare the secretion of the clinical isolate of this project.

As for the tested A549 cell line (lung cancer cells), the reason for the absent effect of infection on cell lysis could simply be that they are less susceptible to bacterial induced cell lysis due to a different immune response.

Summarized it can be said that an infection assay could be established, showing *P. aeruginosa* CF1013 induced cell death in THP1 cells. To evaluate its uses and limitations (e.g. regarding other bacterial strains or cells), further experiments would be needed.

4.2 Ferrostatin-1 does not inhibit *P. aeruginosa* induced cell death

To determine what kind of cell death *P. aeruginosa* CF1013 induces in THP1 cells, ferrostatin-1 was added to the cells. As ferrostatin-1 inhibits ferroptosis [47], addition should result in decreased cell lysis after the infection if the induced cell death was ferroptosis. The results (3.2) however, indicate differently. Ferrostatin-1 as a supplement shows even slightly more lysis than its control with DMSO. This indicates that the cells either do not undergo ferroptosis or another cell death mechanism, most likely pyroptosis, compensates when ferroptosis is inhibited. To investigate possible remaining ferroptosis, pyroptosis had to be excluded. As caspase-1 is a critical enzyme in *P. aeruginosa* induced pyroptosis [96], caspase-1 deficient THP1 cells were used. Those THP1-*defCasp1* cells showed no significant (p = 0.066) difference in lysis comparing infected to not infected control without any supplement. Potentially, this difference might become significant after further replicates of the experiment. This suggests that *P. aeruginosa* CF1013 might induce

at least another form of cell death, since caspase-1 dependent pyroptosis was ruled out by the caspase-1 deficiency [96]. To further examine this observation, another assay comparing the THP1-*null* and the THP1-*defCasp1* cells would be required.

A previous study showed that the inhibition of ABHD12 does not reduce ferroptosis, but increase it in cancer cells [100]. ABHD12 is also a member of the serine hydrolase super family and together with ABHD6 and MAGL, which are examined in this thesis, is responsible for the 2-AG hydrolysis in the human brain [85]. In the context of this thesis, it was tested if the chosen lipase inhibitors showed an impact on cell lysis when infecting THP1-*defCasp1* cells with the clinical isolate of *P. aeruginosa.* None of the inhibitors showed the in the hypothesis expected decrease in lysis, neither did the one with ferrostatin-1. The results of this thesis show that the used lipase inhibitors do not reduce the lytic cell death that is induced by *P. aeruginosa* CF1013 in THP1-*defCasp1* cells. Since these cells lack the relevant enzyme for pyroptosis, caspase-1, ferroptosis would be the suggested cell death. However, since the cell death was not inhibited by ferrostatin-1, it might not be the induced cell death pathway or that in this case another cell death pathway compensates.

It could also be possible that the used concentrations of the inhibitors as well as the concentration of ferrostatin-1 were just not right, as too high or low levels could affect the cells and their lysis differently than expected. However, we used concentrations usually applied in other studies [20, 82, 101-103]. Still, it must be considered that the cell death was caspase-1 dependent pyroptosis as explained above. In this case the lipase inhibitors would probably not interfere with the cell death as pyroptosis is not directly dependent on lipids, which could be investigated in the aforementioned assay of comparison the caspase-1 deficient THP1 cells to the wildtype. Nevertheless, the inhibition of said lipases could still result in elevated levels on 2-AG and decreased levels of arachidonic acid, which has at least been shown in macrophages [85, 86, 89]. Hypothetically this could then on the one hand cause anti-inflammatory and protective effects by 2-AG on the cannabinoid receptors CB_1 and CB_2 [71, 72]. On the other hand a decrease of arachidonic acid could result in less inflammation as arachidonic acid itself as well as its descendants like prostaglandins or other mediators normally contribute a large proportion to the inflammatory reaction in eukaryotic cells during an infection [70]. Ultimately, lysis and therefore cell death could still

be observed and was not decreased or altered in the presence of the tested lipase inhibitors.

The differences in the behavior of the CFU/mL of extracellular load are another observation made in the experiments. While it increases in most experiments with different cells after 2 h and decreases in GM-CSF differentiated human macrophages, it shows hardly any change in THP1-*defCasp1* cells. The increase can most likely and most simply be explained by the fact that the bacteria presumably use the cell culture medium as an energy source and can continue to multiply due to the absence of antibiotics after the majority has been removed following infection. The drop or stagnation in the experiments with hMDMs or THP1-*defCasp1* cells can in turn be attributed to other cellular defense mechanisms, which also require further investigation. Concluding from the points mentioned it can be said that, although no significant influence of lipase inhibitors could be shown in infected THP1 cells, these experiments still contribute to our understanding of biological and physiological processes in eukaryotic cells. The influence of lipids, lipases and their inhibition must be explored further as they still come into question as possible therapeutic targets when it comes to bacterial infections. Since other bacterial strains such as *P. aeruginosa* PP34 have been shown to induce not only pyroptosis but the on peroxidized lipids depending ferroptosis, the inhibition of lipases like MAGL, ATGL or ABHD6 should be further examined in other cells and with other *P. aeruginosa* strains as well.

In conclusion, this study has established an infection assay that can be used to study the lysis of human cells under the influence of *P. aeruginosa*. Furthermore, it was demonstrated that THP1 cells undergo a form of cell death after infection with *P. aeruginosa* that is not suppressed by the applied concentrations of ferrostatin-1 or the investigated lipase inhibitors. Further research is required to investigate the mechanism of the triggered cell death. An infection assay to compare THP1-*null* cells with THP1-*defCasp1* cells, as well as with caspase-4 (and caspase-1) deficient cells, would be a logical next step to further evaluate the induced cell death. In addition, the effects of lipase inhibitors during the infection with other *P. aeruginosa* strains need to be further investigated in order to explore these as potential targets for host-directed therapy.

References

1. Alberts B. JA, Lewis J., et al. Introduction to Pathogenes. Molecular Biology of the Cell. 4th edition ed. New York: Garland Science; 2002.
2. Campbell N, Reece J. Biology. San Francisco: Pearson; 2005.
3. Ryan KJ, Ray CG, Ahmad N, Drew WL, Langunoff M, Pottinger P, et al. Pathogenesis of Bacterial Infections. Sherris Medical Microbiology. 6th edition ed. New York: McGraw Hill Education; 2014. p. 391-406.
4. Tortora GJ, Funke BR, Case CL. Microbiology: An Introduction. Boston: Pearson; 2013.
5. Soni J, Sinha S, Pandey R. Understanding bacterial pathogenicity: a closer look at the journey of harmful microbes. Front Microbiol. 2024;15:1370818.
6. Brown SP, Cornforth DM, Mideo N. Evolution of virulence in opportunistic pathogens: generalism, plasticity, and control. Trends Microbiol. 2012;20(7):336-42.
7. Chinemerem Nwobodo D, Ugwu MC, Oliseloke Anie C, Al-Ouqaili MTS, Chinedu Ikem J, Victor Chigozie U, et al. Antibiotic resistance: The challenges and some emerging strategies for tackling a global menace. J Clin Lab Anal. 2022;36(9):e24655.
8. Classics in infectious diseases. On the blue and green coloration that appears on bandages. By Carle Gessard (1850-1925). Rev Infect Dis. 1984;6 Suppl 3:S775-6.
9. BH. I. Pseudomonas. In: S B, editor. Medical Microbiology. 4th edition ed. Galveston (TX): University of Texas Medical Branch at Galveston; 1996.
10. Spagnolo AM, Sartini M, Cristina ML. Pseudomonas aeruginosa in the healthcare facility setting. Reviews in Medical Microbiology. 2021;32(3):169-75.
11. Tacconelli E, Carrara E, Savoldi A, Harbarth S, Mendelson M, Monnet DL, et al. Discovery, research, and development of new antibiotics: the WHO priority list of antibiotic-resistant bacteria and tuberculosis. Lancet Infect Dis. 2018;18(3):318-27.
12. Diggle SP, Whiteley M. Microbe Profile: Pseudomonas aeruginosa: opportunistic pathogen and lab rat. Microbiology (Reading). 2020;166(1):30-3.
13. Garrity GM, Bell JA, Lilburn T. Pseudomonadales2005.
14. Kenneth T. Todar's Online Textbook of Bacteriology 2020 [Available from: http://textbookofbacteriology.net/pseudomonas.html].
15. Magill SS, Edwards JR, Bamberg W, Beldavs ZG, Dumyati G, Kainer MA, et al. Multistate point-prevalence survey of health care-associated infections. N Engl J Med. 2014;370(13):1198-208.
16. Cross A, Allen JR, Burke J, Ducel G, Harris A, John J, et al. Nosocomial infections due to Pseudomonas aeruginosa: review of recent trends. Rev Infect Dis. 1983;5 Suppl 5:S837-45.
17. Johnson PA. Novel understandings of host cell mechanisms involved in chronic lung infection: Pseudomonas aeruginosa in the cystic fibrotic lung. J Infect Public Health. 2019;12(2):242-6.
18. Sarges E, Rodrigues YC, Furlaneto IP, de Melo MVH, Brabo G, Lopes KCM, et al. Pseudomonas aeruginosa Type III Secretion System Virulotypes and Their Association with Clinical Features of Cystic Fibrosis Patients. Infect Drug Resist. 2020;13:3771-81.
19. Sato H, Frank DW, Hillard CJ, Feix JB, Pankhaniya RR, Moriyama K, et al. The mechanism of action of the Pseudomonas aeruginosa-encoded type III cytotoxin, ExoU. EMBO J. 2003;22(12):2959-69.

20. Bagayoko S, Leon-Icaza SA, Pinilla M, Hessel A, Santoni K, Pericat D, et al. Host phospholipid peroxidation fuels ExoU-dependent cell necrosis and supports Pseudomonas aeruginosa-driven pathology. PLoS Pathog. 2021;17(9):e1009927.
21. El Solh AA, Akinnusi ME, Wiener-Kronish JP, Lynch SV, Pineda LA, Szarpa K. Persistent infection with Pseudomonas aeruginosa in ventilator-associated pneumonia. Am J Respir Crit Care Med. 2008;178(5):513-9.
22. Pankhaniya RR, Tamura M, Allmond LR, Moriyama K, Ajayi T, Wiener-Kronish JP, et al. Pseudomonas aeruginosa causes acute lung injury via the catalytic activity of the patatin-like phospholipase domain of ExoU. Crit Care Med. 2004;32(11):2293-9.
23. Phillips RM, Six DA, Dennis EA, Ghosh P. In vivo phospholipase activity of the Pseudomonas aeruginosa cytotoxin ExoU and protection of mammalian cells with phospholipase A2 inhibitors. J Biol Chem. 2003;278(42):41326-32.
24. Sato H, Frank DW. ExoU is a potent intracellular phospholipase. Mol Microbiol. 2004;53(5):1279-90.
25. Mortensen MS, Ruiz J, Watts JL. Polyunsaturated Fatty Acids Drive Lipid Peroxidation during Ferroptosis. Cells. 2023;12(5).
26. Brett PJ, Deshazer D, Woods DE. Characterization of Burkholderia pseudomallei and Burkholderia pseudomallei-like strains. Epidemiol Infect. 1997;118(2):137-48.
27. Haraga A, West TE, Brittnacher MJ, Skerrett SJ, Miller SI. Burkholderia thailandensis as a model system for the study of the virulence-associated type III secretion system of Burkholderia pseudomallei. Infect Immun. 2008;76(11):5402-11.
28. Yabuuchi E, Kosako Y, Oyaizu H, Yano I, Hotta H, Hashimoto Y, et al. Proposal of Burkholderia gen. nov. and transfer of seven species of the genus Pseudomonas homology group II to the new genus, with the type species Burkholderia cepacia (Palleroni and Holmes 1981) comb. nov. Microbiol Immunol. 1992;36(12):1251-75.
29. Wuthiekanun V, Smith MD, Dance DA, Walsh AL, Pitt TL, White NJ. Biochemical characteristics of clinical and environmental isolates of Burkholderia pseudomallei. J Med Microbiol. 1996;45(6):408-12.
30. Wiersinga WJ, de Vos AF, de Beer R, Wieland CW, Roelofs JJ, Woods DE, et al. Inflammation patterns induced by different Burkholderia species in mice. Cell Microbiol. 2008;10(1):81-7.
31. Morici LA, Heang J, Tate T, Didier PJ, Roy CJ. Differential susceptibility of inbred mouse strains to Burkholderia thailandensis aerosol infection. Microb Pathog. 2010;48(1):9-17.
32. Engelberg-Kulka H, Amitai S, Kolodkin-Gal I, Hazan R. Bacterial programmed cell death and multicellular behavior in bacteria. PLoS Genet. 2006;2(10):e135.
33. Festjens N, Vanden Berghe T, Vandenabeele P. Necrosis, a well-orchestrated form of cell demise: signalling cascades, important mediators and concomitant immune response. Biochim Biophys Acta. 2006;1757(9-10):1371-87.
34. Nirmala JG, Lopus M. Cell death mechanisms in eukaryotes. Cell Biol Toxicol. 2020;36(2):145-64.
35. Proskuryakov SY, Konoplyannikov AG, Gabai VL. Necrosis: a specific form of programmed cell death? Exp Cell Res. 2003;283(1):1-16.
36. Ruffolo PR. THE PATHOGENESIS OF NECROSIS. I. CORRELATED LIGHT AND ELECTRON MICROSCOPIC OBSERVATIONS OF THE MYOCARDIAL NECROSIS INDUCED BY THE INTRAVENOUS INJECTION OF PAPAIN. Am J Pathol. 1964;45(5):741-56.

37. Bohm I, Schild H. Apoptosis: the complex scenario for a silent cell death. Mol Imaging Biol. 2003;5(1):2-14.
38. Bertheloot D, Latz E, Franklin BS. Necroptosis, pyroptosis and apoptosis: an intricate game of cell death. Cell Mol Immunol. 2021;18(5):1106-21.
39. Chen G, Goeddel DV. TNF-R1 signaling: a beautiful pathway. Science. 2002;296(5573):1634-5.
40. Ketelut-Carneiro N, Fitzgerald KA. Apoptosis, Pyroptosis, and Necroptosis-Oh My! The Many Ways a Cell Can Die. J Mol Biol. 2022;434(4):167378.
41. Lockshin RA, Zakeri Z. Programmed cell death and apoptosis: origins of the theory. Nat Rev Mol Cell Biol. 2001;2(7):545-50.
42. Tonnus W, Meyer C, Paliege A, Belavgeni A, von Massenhausen A, Bornstein SR, et al. The pathological features of regulated necrosis. J Pathol. 2019;247(5):697-707.
43. Tan S, Schubert D, Maher P. Oxytosis: A novel form of programmed cell death. Curr Top Med Chem. 2001;1(6):497-506.
44. Yang WS, Stockwell BR. Ferroptosis: Death by Lipid Peroxidation. Trends Cell Biol. 2016;26(3):165-76.
45. Stockwell BR, Friedmann Angeli JP, Bayir H, Bush AI, Conrad M, Dixon SJ, et al. Ferroptosis: A Regulated Cell Death Nexus Linking Metabolism, Redox Biology, and Disease. Cell. 2017;171(2):273-85.
46. Maher P, Currais A, Schubert D. Using the Oxytosis/Ferroptosis Pathway to Understand and Treat Age-Associated Neurodegenerative Diseases. Cell Chem Biol. 2020;27(12):1456-71.
47. Dixon SJ, Lemberg KM, Lamprecht MR, Skouta R, Zaitsev EM, Gleason CE, et al. Ferroptosis: an iron-dependent form of nonapoptotic cell death. Cell. 2012;149(5):1060-72.
48. Bagayoko S, Meunier E. Emerging roles of ferroptosis in infectious diseases. FEBS J. 2022;289(24):7869-90.
49. Lu B, Chen XB, Ying MD, He QJ, Cao J, Yang B. The Role of Ferroptosis in Cancer Development and Treatment Response. Front Pharmacol. 2017;8:992.
50. Sun Y, Chen P, Zhai B, Zhang M, Xiang Y, Fang J, et al. The emerging role of ferroptosis in inflammation. Biomed Pharmacother. 2020;127:110108.
51. Weiland A, Wang Y, Wu W, Lan X, Han X, Li Q, et al. Ferroptosis and Its Role in Diverse Brain Diseases. Mol Neurobiol. 2019;56(7):4880-93.
52. Jorgensen I, Miao EA. Pyroptotic cell death defends against intracellular pathogens. Immunol Rev. 2015;265(1):130-42.
53. Broz P, Dixit VM. Inflammasomes: mechanism of assembly, regulation and signalling. Nat Rev Immunol. 2016;16(7):407-20.
54. Broz P, Monack DM. Newly described pattern recognition receptors team up against intracellular pathogens. Nat Rev Immunol. 2013;13(8):551-65.
55. Mariathasan S, Newton K, Monack DM, Vucic D, French DM, Lee WP, et al. Differential activation of the inflammasome by caspase-1 adaptors ASC and Ipaf. Nature. 2004;430(6996):213-8.
56. Lichtenegger S, Stiehler J, Saiger S, Zauner A, Kleinhappl B, Bernecker C, et al. Burkholderia pseudomallei triggers canonical inflammasome activation in a human primary macrophage-based infection model. PLoS Negl Trop Dis. 2020;14(11):e0008840.
57. Yu P, Zhang X, Liu N, Tang L, Peng C, Chen X. Pyroptosis: mechanisms and diseases. Signal Transduct Target Ther. 2021;6(1):128.

58. Diamond CE, Khameneh HJ, Brough D, Mortellaro A. Novel perspectives on non-canonical inflammasome activation. Immunotargets Ther. 2015;4:131-41.
59. Agmon E, Stockwell BR. Lipid homeostasis and regulated cell death. Curr Opin Chem Biol. 2017;39:83-9.
60. Bleicken S, Hantusch A, Das KK, Frickey T, Garcia-Saez AJ. Quantitative interactome of a membrane Bcl-2 network identifies a hierarchy of complexes for apoptosis regulation. Nat Commun. 2017;8(1):73.
61. Flores-Romero H, Landeta O, Ugarte-Uribe B, Cosentino K, Garcia-Porras M, Garcia-Saez AJ, et al. BFL1 modulates apoptosis at the membrane level through a bifunctional and multimodal mechanism showing key differences with BCLXL. Cell Death Differ. 2019;26(10):1880-94.
62. Kuwana T, Mackey MR, Perkins G, Ellisman MH, Latterich M, Schneiter R, et al. Bid, Bax, and lipids cooperate to form supramolecular openings in the outer mitochondrial membrane. Cell. 2002;111(3):331-42.
63. Magtanong L, Ko PJ, Dixon SJ. Emerging roles for lipids in non-apoptotic cell death. Cell Death Differ. 2016;23(7):1099-109.
64. Gonzalvez F, Pariselli F, Dupaigne P, Budihardjo I, Lutter M, Antonsson B, et al. tBid interaction with cardiolipin primarily orchestrates mitochondrial dysfunctions and subsequently activates Bax and Bak. Cell Death Differ. 2005;12(6):614-26.
65. Gonzalvez F, Schug ZT, Houtkooper RH, MacKenzie ED, Brooks DG, Wanders RJ, et al. Cardiolipin provides an essential activating platform for caspase-8 on mitochondria. J Cell Biol. 2008;183(4):681-96.
66. Jalmar O, Francois-Moutal L, Garcia-Saez AJ, Perry M, Granjon T, Gonzalvez F, et al. Caspase-8 binding to cardiolipin in giant unilamellar vesicles provides a functional docking platform for bid. PLoS One. 2013;8(2):e55250.
67. Dixon SJ. Ferroptosis: bug or feature? Immunol Rev. 2017;277(1):150-7.
68. Forcina GC, Dixon SJ. GPX4 at the Crossroads of Lipid Homeostasis and Ferroptosis. Proteomics. 2019;19(18):e1800311.
69. Flores-Romero H, Ros U, Garcia-Saez AJ. A lipid perspective on regulated cell death. Int Rev Cell Mol Biol. 2020;351:197-236.
70. Wlodawer P, Samuelsson B. On the Organization and Mechanism of Prostaglandin Synthetase. Journal of Biological Chemistry. 1973;248(16):5673-8.
71. Stella N, Schweitzer P, Piomelli D. A second endogenous cannabinoid that modulates long-term potentiation. Nature. 1997;388(6644):773-8.
72. Sugiura T, Kodaka T, Nakane S, Miyashita T, Kondo S, Suhara Y, et al. Evidence that the cannabinoid CB1 receptor is a 2-arachidonoylglycerol receptor. Structure-activity relationship of 2-arachidonoylglycerol, ether-linked analogues, and related compounds. J Biol Chem. 1999;274(5):2794-801.
73. Johnson AG, Wein T, Mayer ML, Duncan-Lowey B, Yirmiya E, Oppenheimer-Shaanan Y, et al. Bacterial gasdermins reveal an ancient mechanism of cell death. Science. 2022;375(6577):221-5.
74. Fruhbeck G, Mendez-Gimenez L, Fernandez-Formoso JA, Fernandez S, Rodriguez A. Regulation of adipocyte lipolysis. Nutr Res Rev. 2014;27(1):63-93.
75. Hofer P, Taschler U, Schreiber R, Kotzbeck P, Schoiswohl G. The Lipolysome-A Highly Complex and Dynamic Protein Network Orchestrating Cytoplasmic Triacylglycerol Degradation. Metabolites. 2020;10(4).

76. Karlsson M, Contreras JA, Hellman U, Tornqvist H, Holm C. cDNA cloning, tissue distribution, and identification of the catalytic triad of monoglyceride lipase. Evolutionary relationship to esterases, lysophospholipases, and haloperoxidases. J Biol Chem. 1997;272(43):27218-23.
77. Lehner R, Quiroga AD. Fatty Acid Handling in Mammalian Cells. Biochemistry of Lipids, Lipoproteins and Membranes2016. p. 149-84.
78. Ojha S, Budge H, Symonds ME. Adipocytes in Normal Tissue Biology. Pathobiology of Human Disease2014. p. 2003-13.
79. Zhang X, Heckmann BL, Liu J. Studying lipolysis in adipocytes by combining siRNA knockdown and adenovirus-mediated overexpression approaches. Methods Cell Biol. 2013;116:83-105.
80. Bongarzone Ernesto R., Givogri Maria I., De Vivo Darryl C., Salvatore D. Eighth Edition Acknowledgments and History. Basic Neurochemistry2012.
81. Young SG, Zechner R. Biochemistry and pathophysiology of intravascular and intracellular lipolysis. Genes Dev. 2013;27(5):459-84.
82. Mayer N, Schweiger M, Romauch M, Grabner GF, Eichmann TO, Fuchs E, et al. Development of small-molecule inhibitors targeting adipose triglyceride lipase. Nat Chem Biol. 2013;9(12):785-7.
83. Blankman JL, Simon GM, Cravatt BF. A comprehensive profile of brain enzymes that hydrolyze the endocannabinoid 2-arachidonoylglycerol. Chem Biol. 2007;14(12):1347-56.
84. Marrs WR, Blankman JL, Horne EA, Thomazeau A, Lin YH, Coy J, et al. The serine hydrolase ABHD6 controls the accumulation and efficacy of 2-AG at cannabinoid receptors. Nat Neurosci. 2010;13(8):951-7.
85. Savinainen JR, Saario SM, Laitinen JT. The serine hydrolases MAGL, ABHD6 and ABHD12 as guardians of 2-arachidonoylglycerol signalling through cannabinoid receptors. Acta Physiol (Oxf). 2012;204(2):267-76.
86. Alhouayek M, Masquelier J, Cani PD, Lambert DM, Muccioli GG. Implication of the anti-inflammatory bioactive lipid prostaglandin D2-glycerol ester in the control of macrophage activation and inflammation by ABHD6. Proc Natl Acad Sci U S A. 2013;110(43):17558-63.
87. Hsu KL, Tsuboi K, Chang JW, Whitby LR, Speers AE, Pugh H, et al. Discovery and optimization of piperidyl-1,2,3-triazole ureas as potent, selective, and in vivo-active inhibitors of alpha/beta-hydrolase domain containing 6 (ABHD6). J Med Chem. 2013;56(21):8270-9.
88. Li W, Blankman JL, Cravatt BF. A functional proteomic strategy to discover inhibitors for uncharacterized hydrolases. J Am Chem Soc. 2007;129(31):9594-5.
89. Dinh TP, Carpenter D, Leslie FM, Freund TF, Katona I, Sensi SL, et al. Brain monoglyceride lipase participating in endocannabinoid inactivation. Proc Natl Acad Sci U S A. 2002;99(16):10819-24.
90. Long JZ, Li W, Booker L, Burston JJ, Kinsey SG, Schlosburg JE, et al. Selective blockade of 2-arachidonoylglycerol hydrolysis produces cannabinoid behavioral effects. Nat Chem Biol. 2009;5(1):37-44.
91. A549 Cells [ATCC:[Available from: https://www.atcc.org/products/ccl-185]].
92. Giard DJ, Aaronson SA, Todaro GJ, Arnstein P, Kersey JH, Dosik H, et al. In vitro cultivation of human tumors: establishment of cell lines derived from a series of solid tumors. J Natl Cancer Inst. 1973;51(5):1417-23.

93. THP1-Null Cells 2016 [InvivoGen:[Available from: https://www.invivogen.com/thp1-null]].
94. Tsuchiya S, Yamabe M, Yamaguchi Y, Kobayashi Y, Konno T, Tada K. Establishment and characterization of a human acute monocytic leukemia cell line (THP-1). Int J Cancer. 1980;26(2):171-6.
95. THP1-defCASP1 Cells 2016 [InvivoGen:[Available from: https://www.invivogen.com/thp1-defcasp1]].
96. Man SM, Kanneganti TD. Converging roles of caspases in inflammasome activation, cell death and innate immunity. Nat Rev Immunol. 2016;16(1):7-21.
97. Firouzi-Dalvand L PM, Nowroozi J, Akhvan-Sepahi A, Hooshiyar M. Presence of *exoU* and *exoS* Genes in *Pseudomonas aeruginosa* Isolated from Urinary Tract Infections. Infection, Epidemiology and Medicine. 2016;2(2):8-11.
98. Stolt C, Schmidt IH, Sayfart Y, Steinmetz I, Bast A. Heme Oxygenase-1 and Carbon Monoxide Promote Burkholderia pseudomallei Infection. J Immunol. 2016;197(3):834-46.
99. Dasgupta N, Ashare A, Hunninghake GW, Yahr TL. Transcriptional induction of the Pseudomonas aeruginosa type III secretion system by low Ca2+ and host cell contact proceeds through two distinct signaling pathways. Infect Immun. 2006;74(6):3334-41.
100. Kathman SG, Boshart J, Jing H, Cravatt BF. Blockade of the Lysophosphatidylserine Lipase ABHD12 Potentiates Ferroptosis in Cancer Cells. ACS Chem Biol. 2020;15(4):871-7.
101. Bottemanne P, Paquot A, Ameraoui H, Alhouayek M, Muccioli GG. The alpha/beta-hydrolase domain 6 inhibitor WWL70 decreases endotoxin-induced lung inflammation in mice, potential contribution of 2-arachidonoylglycerol, and lysoglycerophospholipids. FASEB J. 2019;33(6):7635-46.
102. Sathyanarayan A, Mashek MT, Mashek DG. ATGL Promotes Autophagy/Lipophagy via SIRT1 to Control Hepatic Lipid Droplet Catabolism. Cell Rep. 2017;19(1):1-9.
103. Tardelli M, Bruschi FV, Fuchs CD, Claudel T, Auer N, Kunczer V, et al. Monoacylglycerol Lipase Inhibition Protects From Liver Injury in Mouse Models of Sclerosing Cholangitis. Hepatology. 2020;71(5):1750-65.

For the main purpose of translation as well as for paraphrasing, improving clarity and readability of the provided text, the AI tool DeepL Translator and DeepL Write (both DeepL SE) were used by the author. All AI generated text was thoroughly proofread and corrected were necessary to ensure accuracy and alignment with the original meaning. The author takes full responsibility for the final work.